Borrelia burgdorferi ErpB and ErpQ Inhibit C1 Complex of the Classical Pathway of Complement Through a Novel Mechanism

by

Ryan Garrigues

May 2021

Director of Thesis: Brandon Garcia, PhD

Major Department: Biomedical Sciences

The complement system is an organized proteolytic cascade of dozens of proteins that functions in the recognition, opsonization, and lysis of pathogenic and altered-host cells. Bloodborne pathogens like the etiologic agent of Lyme disease, *Borrelia burgdorferi,* encounter complement during their bloodmeal and in their dissemination through the body. Therefore, to avoid complement mediated destruction, these pathogens have developed mechanisms that aid in complement evasion and defense. The spirochete *B. burgdorferi*, has nearly a dozen known complement recruiting or inhibiting surface exposed lipoproteins. Here, we uncover a novel inhibitory mechanism for two surface exposed lipoproteins, ErpB and ErpQ, that were recently identified using a lipoprotein gain of function library. Using surface plasmon resonance, ErpB and ErpQ were found to bind C1 complex proteases C1r and C1s with high affinity. Gel-based biochemical assays showed that ErpB and ErpQ specifically inhibit C1s-mediated cleavage of

both C2 and C4 making them the only known bacterial inhibitors of C1s. Furthermore, they were shown to block C1s outside of the active site indicating that they function by a novel mechanism. Additional site-directed mutagenesis of C1s exosites revealed determinants for high affinity inhibitor interactions that have been shown to be important for C1s recognition of C4 outside of the active site.

The discovery of a novel mechanism of complement inhibition by a medically-relevant human pathogen expands our knowledge of host pathogens interactions and contributes to previously unknown pathophysiological immune evasion by *B. burgdorferi*. Mechanistic studies on ErpB and ErpQ also support further understanding of molecular interactions between complement proteases and their substrates, which provides alternative means for the development of specific complement therapeutics toward complement-mediated diseases.

Borrelia burgdorferi **ErpB and ErpQ Inhibit C1 Complex of the Classical Pathway of**

Complement Through a Novel Mechanism

A Thesis

Presented to the Faculty of the Biomedical Sciences Program

Brody School of Medicine at East Carolina University

In Partial Fulfillment of the Requirements for the Degree

Master of Science in Biomedical Sciences

by

Ryan Garrigues

May 2021

Borrelia burgdorferi **ErpB and ErpQ Inhibit C1 Complex of the Classical Pathway of**

Complement Through a Novel Mechanism

by

Ryan Garrigues

APPROVED BY:

DIRECTOR OF THESIS: _____
Brandon L. Garcia, PhD

COMMITTEE MEMBER: _____
Daniel W. Martin, PhD

COMMITTEE MEMBER: _____
Tonya N. Zeczycki, PhD

COMMITTEE MEMBER: _____
MD A. Motaleb, PhD

PROGRAM DIRECTOR OF

BIOMEDICAL SCIENCE PROGRAM: _____
Richard A. Franklin, PhD

DEAN OF THE GRADUATE SCHOOL: _____
Paul J. Gemperline, PhD

Table of Contents

List of Tables

List of Figures

CHAPTER 1: Introduction

The Complement System

The complement system is an ancient proteolytic cascade that participates in the surveillance and destruction of pathogenic and altered-self cells. Consisting of dozens of proteins, the complement system comprises three interrelated, but differentially activated pathways, the classical pathway (CP), lectin pathway (LP) and alternative pathway (AP)[1,2] (**Fig 1**). Each pathway differs by the source of activation and is differentiated primarily by pattern recognition molecules (PRM) that function to identify foreign or altered moieties on cell surfaces. The potent effector functions of complement activation make it a prime target for global and local regulation at the site of stimulation[3]. Altogether the functional aspects of complement activation make it a unique and important addition to the innate immune system.

The classical pathway is initiated by the recognition of immune complexes through the first component of complement C1. C1 is a large 766 kDa complex made of three subcomponents: i) a hexameric collagen-like recognition molecule with six globular domains known as C1q, and ii) a heterotetramer of the serine proteases $C1r_2$ and $C1s_2$[4–6]. Upon recognition of immune complexes, a dramatic conformational change in the C1 complex (i.e. $C1qC1r_2C1s_2$) is induced and allows zymogen C1r to become activated through an autocatalytic mechanism. Subsequent cleavage of proenzyme C1s by C1r enzyme ensues to fully activate C1. C1s enzyme then proteolytically cleaves complement component C4 into two components, a soluble C4a and C4b which covalently reacts to nearby surfaces via a thioester bond. C4b promotes binding of C2 which is subsequently cleaved by C1s into C2b, the C4b membrane bound fraction, and C2a which acts as a mild anaphylatoxin[7-8]. The lectin pathway, described below, converges with the formation of this C4b2b complex.

The lectin pathway recognizes foreign carbohydrate surfaces, primarily terminal mannose residues, by its PRMs mannose-binding lectin (MBL), collectins, and ficolins[9]. Subsequent activation of the pathway occurs through MBL associated serine proteases (MASPs), which bind to MBL forming MBL/MASP complexes. MASP-1 is thought to be the activator of the LP through a mechanism of auto activation and subsequently cleaves adjacent MASP-2 complexes[10]. Activated proteases MASP-1 and MASP-2 cleave complement component C4, which like C1s, produces membrane bound C4b and solution-phase C4a[11]. C4b then binds C2 which is promptly cleaved by MASP-2 into C2b, the C4b bound fraction, and C2a. The formation of the C4b2b, a C3 convertase, represents the convergence of the CP with the LP (**Fig 1**).

The alternative pathway does not recognize surface patterns of cells, rather is constitutively active under normal conditions through a process known as "tick-over." This mechanism for activation is underpinned by the unique nature of the initiating molecule of the AP, complement component C3, to be spontaneously hydrolyzed by water into C3 (H_2O). Subsequent recognition of C3(H_2O) by factors B and D (FB and FD, respectively) to C3(H_2O)Bb can opsonize surfaces in proximity[12]. Upon opsonization the C3(H_2O)Bb complex acts as a C3 convertase cleaving nearby C3 molecules, forming an amplification loop to fully opsonize the target and elicit the formation of the AP C3 convertase C3bBb. Through proper activation this amplification loop on appropriate surfaces is not easily stopped by complement regulators and works as a positive feedback loop. Though differentially activated the three pathways converge at the level of the C3 convertase, therefore proceeding activation steps and termination of all three pathways are amplified by the AP[1].

Cooperatively these pathways initiate the formation of the C3 convertase to promote

cleavage of C3. Cleavage of C3 into C3a, a potent anaphylatoxin towards the recruitment of

neutrophils and macrophages, and C3b, which is added to C3 convertases, C4b2b and C3bBb,

respectively to create C5 convertases. C5 is then cleaved into soluble anaphylatoxin, C5a, and

C5b which binds to the target surface and recruits C6, C7, C8, and $C9_n$, creating the membrane

attack complex (MAC). MAC is a large porin-like structure that functions to disrupt membrane

potential causing cell lysis[1,13]. The effector functions of the complement system contain

inflammatory and destructive properties, which gone unregulated cause a multitude of

pathologies. Therefore, there is a critical need for pathway specific and global mechanisms of

regulation[1,3,14].

Regulators of Complement Activity

To avoid activation of complement on healthy host cells, close regulation of complement

is carried out by both membrane bound and soluble regulatory factors, collectively known as

regulators of complement activity (RCA)[15]. Functional redundancy in this way allows for

multiple levels of control over different activation pathways as well as different conditions in the

milieu. Regulatory control is placed at three main steps in the cascade: activation, amplification,

and termination.

The activation of the classical and lectin pathways is controlled by several proteins

through both direct inhibition and cofactor recruitment. Direct inhibition of the CP and LP is

achieved through C1 esterase inhibitor (C1-INH)[4,16,17]. C1-INH is a member of the serine

protease inhibitor (SERPIN) family of protease inhibitors, whose mechanism involves

noncompetitive covalent neutrophilic attack of the catalytic serine[18,19]. This covalent attack

irreversibly inhibits protease function and prevents further downstream proteolytic events. C1-

INH is unique as it is capable of complexing with C1r, C1s, MASP-1, MASP-2, and several coagulation proteases as well as functioning to dislodge the proteases from C1 complex. Moreover, C1-INH is known to make noncovalent interactions with the C1 complex, which are independent of its final inhibitory state[20]. In addition to its regulation over the complement cascade, C1-INH has effector functions over the contact and fibrinolytic systems making it a promiscuous regulator of blood proteases. More recently, roles for proteins ApoE4 and SRPX2 have shown that there are other methods for immune regulation of complement in immune privileged sites like the brain[21,22]. Though these inhibitors have been implicated in their association with a C1q-related mechanism of action rather than direct protease interaction making them distinct regulators of the CP. Although more research is needed to determine the molecular mechanisms of each of these proteins is needed.

Amplification of the complement cascade occurs through the formation of C3 convertases, which each produce more C3 convertases through the alternative pathway. To prevent overactivation of these convertases, the complement system employs a variety of regulators that control the CP/LP and/or the AP. Regulation of the convertases happens at several levels, chiefly they are impacted by negative regulators which work to disassemble them on host surfaces. The first defense in formation of the convertases comes in the form of structural deficiencies, which make the convertases extremely labile and unstable with a half-life of <1 min at 37° C[23,24]. The apparent instability of the complex allows for the complement system to employ decay accelerating factor (DAF), which functions to catalyze the destabilization of the convertases as a negative regulator[15,25]. In addition to DAF, factor H is a long 20 complement control protein (CCP) containing macromolecule which also has decay accelerating factor ability, as well as the ability to recruit factor I (FI) for inactivation through cofactor ability[26]. FI

is a serine protease which functions to cleave C3b and C4b into inactive fragments iC3b and

C4d, respectively. This occurs to destabilize C3 convertases to limit activation on competent host

surfaces and ameliorate aberrant activation of complement. As cofactors to FI, factor H (FH), C4

binding protein (C4BP) is an octopus-like molecule that recognizes the S protein on host cells

and binds deposited C4b and recruits FI. Complement receptor 1 (CR1, CD35) and membrane

cofactor protein (MCP, CD46) are membrane bound receptors that recognize C3b and C4b that

are deposited on the surface, subsequently they recruit FI for inactivation[27].

Ultimately the most dangerous step in the activation of complement, must also be

controlled to deter unintended host cell lysis by the formation of MAC. Clusterin (CLU) and

vitronectin (Vn) were found to impede the development by binding to hydrophobic interaction

domains in components C7, C8, and C9. By binding these moieties, CLU and Vn effectively

solubilize these components into the environment away from the activating surface[28,29]. The

glycosylphosphatidylinositol-linked (GPI-linked) CD59, also known as the MAC inhibitory

protein, is a membrane bound negative regulator that interacts with C9 and prevents

polymerization[30] (**Fig 1**).

Under normal homeostatic conditions the activation and regulation of complement is

tightly controlled and represents a major arm of the innate immune system functioning in the

surveillance, opsonization, and clearance of foreign cells. Coupled with the effector functions of

complement, the system also informs adaptive immune responses with soluble anaphylatoxins

C3a and C5a, which each act as powerful cytokines[3,14]. Their functions include mediating

chemotaxis as potent chemoattractant toward mast cells, neutrophils, and monocytes, as well as

directly function to elicit degranulation and vasodilation important for the destruction of cells

and improvement of vascular permeability around the site of acute inflammation[3].
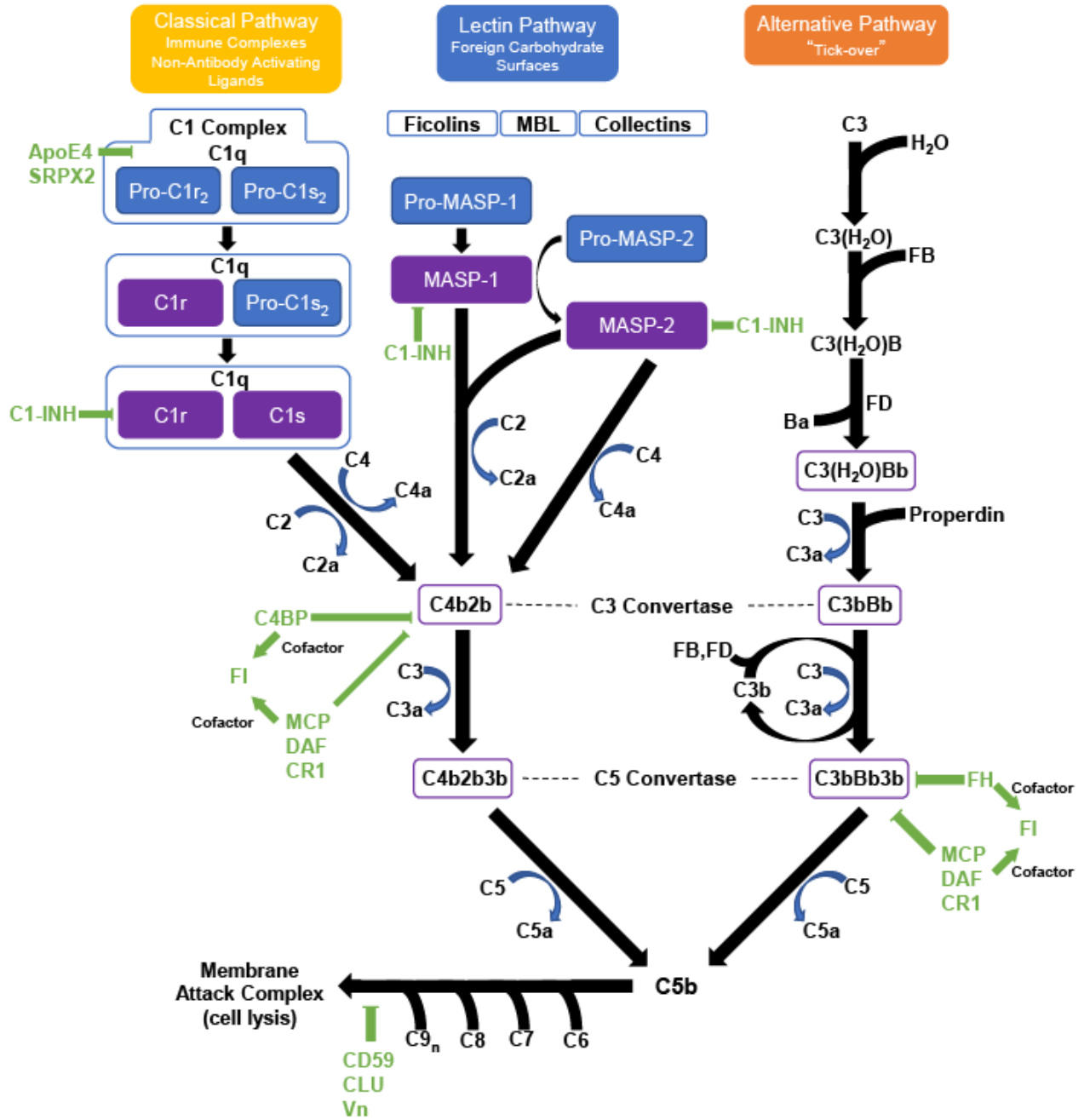
Figure 1. Scheme of complement activation and regulation in the host. Activation of the three initiating pathways of complement with zymogen proenzymes denoted 'Pro' (blue) and with active enzymes (purple). Proteolytic cleavage of complement components is nonreversible and therefore multiple redundant mechanisms for regulation (green) are needed. All three pathways converge at the level of the C3 convertase with further procession eliciting the porin effector, membrane attack complex, which causes loss of membrane potential and elicits cells lysis. Abbreviations: ApoE4, Apolipoprotein E4; SRPX2, Sushi Repeat Containing Protein X-Linked 2, SRPX2; MBL, mannose-binding lectin; MASP, MBL associated serine protease; C1-INH, C1 esterase inhibitor; C4BP, C4 binding protein; FI, factor I; MCP, membrane cofactor protein; DAF, decay accelerating factor; CR1, complement receptor 1; FB, factor B; FD, factor D; FH, factor H.

Lyme Disease

In the 1960's and 70's children of Old Lyme, CT were found to be experiencing symptoms of childhood arthritis, chronic fatigue, and skin rashes. This alarmed the community and lead two mothers to become patient advocates gathering information from affected families. They noticed that all children had experienced tick bites shortly before ailment, it was then that research community started documenting cases of what they called Lyme Arthritis[31]. It was not until 1982 that a researcher named Willy Burgdorfer, who studied rocky mountain spotted fever, described the now established etiologic agent of Lyme Disease, *Borrelia burgdorferi*[32,33]. Further research efforts have identified many more species that make up the Lyme Disease spirochetes making up the newly proposed gen. nov. *Borreliella*[34–36].

Borreliella are a gram-negative extracellular pathogens known for its distinct spirochetal morphology, which is unique in its method of motility through a system of between 7-11

periplasmic flagella[37]. The vector borne spirochete is transmitted through the bloodmeal of an infected *Ixodes spp.* tick. Sterile naïve tick larvae first encounter infected reservoir hosts such as the white-footed mouse, *Peromyscus leucopus*, and become infected[38].
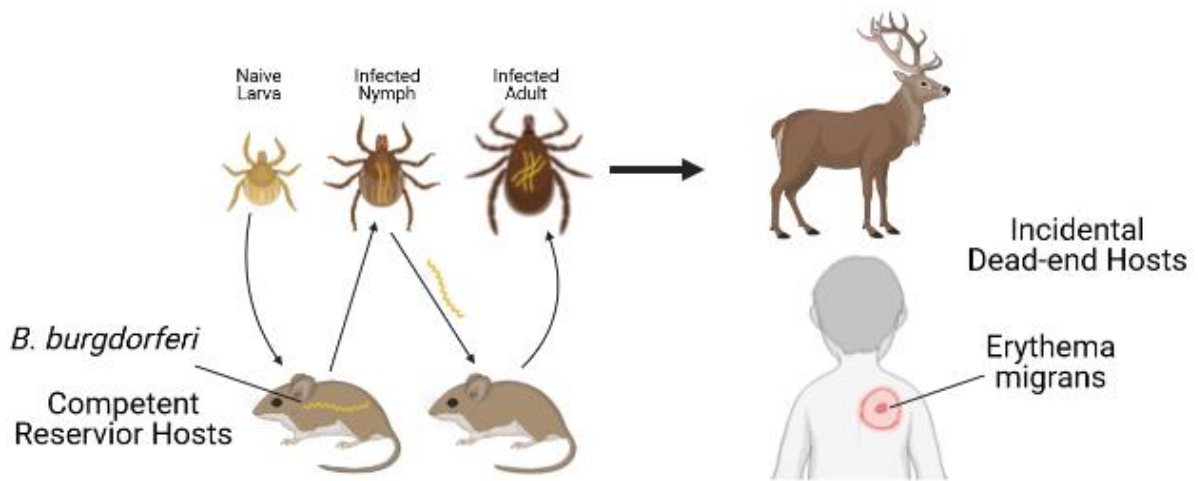
Figure 2. *Borrelia burgdorferi* transmission through tick life cycle. The life cycle of the tick begins with the birth of naïve spirochete-free larvae. Upon first feeding with reservoir hosts such as birds, squirrels, or mice larva then become infected. Ticks then molt to become nymphs, which can infect competent reservoir hosts. The tick then molts again to become an adult, which feeds on a third host, often this host is larger such as a deer to promote mating. Figure was created with Biorender.com.

After a second feeding with other small reservoir hosts as a nymph, which can infect these animals, ticks then feed on larger hosts such as deer, wolves, or humans. These incidental hosts are unable to transmit the spirochete back to naïve ticks and are therefore known as dead-end hosts[38] **(Fig. 2)**. Transmission to humans results in Lyme disease.

Primary presentation of the illness is associated with the formation of erythema migrans, a characteristic bull's eye rash, which represents the dissemination of bacteria near the surface of

the skin **(Fig. 2)**. Later stages include dissemination of *Borreliella* in various host tissues including the joints, heart, and central nervous system[39]. To disseminate into these tissues, *Borreliella* enters the vasculature and like many hematogenous organisms must have mechanisms for the evasion of the host immune system.

Borreliella infection can be treated with a 14-day course of Doxycycline, Amoxicillin, or Cefuroxime. However, patients have also developed an autoimmune response to *B. burgdorferi* which is known as Post-Treatment Lyme Disease Syndrome (PTLDS)[40]. Unfortunately, despite many years of research, detection methods for early *Borreliella* infection are inefficient and there is no vaccine for Lyme disease at this time[41]. With over 470,000 expected new cases per year in the US and over 47,000 reported cases, Lyme disease leads as the number one vector-borne disease and places fifth on the list of highest notifiable infections list[42].

Redundant Mechanisms of Complement Evasion by Borreliella

Upon transmission to the host via a bloodmeal, *Borreliella* spirochetes are inundated with complement attack and therefore need mechanisms to avoid complement-mediated lysis. Notably *Borreliella* encodes an extensive catalog of redundant proteins that target and inhibit several levels of complement activation. To date 11 proteins have been characterized as complement inhibitors in two categories: direct inhibition and complement regulatory acquiring surface proteins (CRASPs)[43–45]. Nine of these have been described in *B. burgdorferi* making up nearly 11% of the total known surface lipoproteome. This functional and diverse redundancy of inhibition has allowed *B. burgdorferi* to become a model organism for complement evasion. However due to the challenging genetic makeup of *Borrelia* spp., it has been difficult to ascertain reasons underlying the high level of redundancy[44,46].
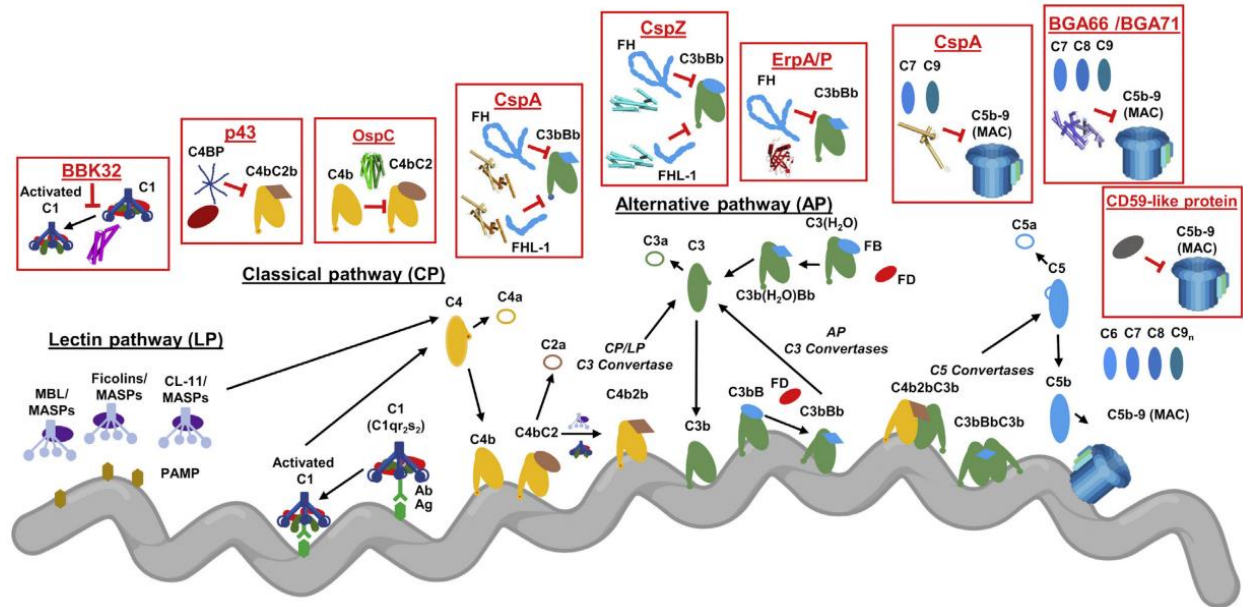
Figure 3. Known Borreliella complement evasion proteins. Inhibition of complement by *Borreliella* spirochetes is a highly redundant process making up a significant portion of the outer surface lipoproteome. Direct and indirect mechanisms of complement evasion are achieved though inhibition of proteolytic activity, recruitment of RCA, and direct inhibition of MAC. Figure reproduced from[44].

Direct complement inhibition occurs through four characterized but mechanistically distinct proteins all of which have been shown to be upregulated upon entrance into the host. OspC was shown to inhibit both the CP and LP through binding of C4b and sterically occluding the binding of component C2, thus inhibiting downstream effectors of two pathways before the formation of the CP/LP convertase. CspA, BGA66/BGA71 (made by *B. bavariensis)*, and CD59-like molecule have been described to direct inhibit MAC through binding of components C7 and C9 and preventing C9 polymerization[47–49]. However, the CD59-like molecule has not been associated with a gene to date[49]. Finally, BBK32 has been found to have complement inhibitory capabilities restricted to the C-terminus[50,51]. The mechanism for classical pathway inhibition of

complement was recently described and remains the only microbial inhibitor of C1r through occlusion of the active site[52].

As described earlier, the complement system exhibits multiple levels of regulation to control inappropriate or aberrant activation. Another method of evasion used by *B. burgdorferi* is the recruitment of these RCAs to the surface using CRASPs. These CRASPs fall into 2 categories: FH/FHL-1 (factor H-like) binding or C4BP binding. Both of which highjack the host negative regulation components to evade complement effector functions. CspA, CspZ, and ErpC are capable of binding both FH and FHL-1 to negatively regulate the formation of the C3 convertase[53,54]. FH binds FI, which proteolytically degrades C3b into an inactive form iC3b, alternatively it also contains decay accelerating factor abilities which disassociate the AP C3 convertase C3Bb into C3b[53,55]. The role of CspA here is multifunctional in that its ability to inhibit the formation of MAC is independent of its ability to bind and utilize FH. CRASPs ErpA and ErpP, are able to bind FH to utilize its negative regulatory ability but are unable to bind the highly similar FHL-1. Recruitment of yet another negative regulator C4BP is performed by borrelial p43, which then recruits FI. FI then proteolytically cleaves C4b into inactive iC4b, thus inhibiting the downstream effects of both the CP and LP.

Although the genetic makeup and functional redundancy of complement inhibition make it difficult to determine the importance of each individual inhibitor. *In vivo* studies of the importance of complement protection have been reported in mice deficient in C1q and C3 with each deficiency resulting in higher bacterial loads[56–58]. Alternatively, mice deficient in FH, FB, or C5 exhibited only modest differences in pathogenesis placing more emphasis on the classical pathway and adaptive immune response[43,59,60]. Altogether these proteins represent a variety of

redundant mechanisms that protect *B. burgdorferi* from complement mediated harm making them contributors to pathogenesis.

OspE/F Related Protein Family

Paralogous gene families are proteins of the same genetic origin existing in the same species often contributing similar functions and are a common feature in the proteome of *Borreliella*[61,62]. As a result of the work completed by Dowdell et al. (discussed further in the next section), it is now known that *B. burgdorferi* B31 expresses several of these paralogous families including Mlp, Rev, and Erp proteins on the surface [46,62]. The Osp<u>E</u>/F <u>r</u>elated <u>p</u>rotein (Erp) family of proteins have been shown to be expressed upon entrance into hosts, and identified as highly immunogenic makers for the host immune response[63–65]. However, a small sub-group of these Erp paralogs are distinguished from the larger family by their similarity in their leader peptides[66]. These Osp<u>E</u>/F-like <u>l</u>eader <u>p</u>eptide (Elp) proteins make up an assortment of Erp proteins including Erps B, O, M, Q and X[65,66]. Although other paralogous Erps A, C, and P have been shown to interact with complement little is known about the function of other Erp/Elp proteins[45].

Gain of Function Library Identifies C1 Interacting Molecules

Previously it has been difficult to determine outer surface lipoproteins contributions to virulence in *B. burgdorferi* as the lipoproteome was not fully known. Recently Dowdell et al. exhaustively described the outer surface lipoproteome using a gain of function protein expression system in a highly passaged non-infectious strain B31e-2[46]. This study individually expressed each of the proposed 127 lipoproteins in *B. burgdorferi* and assessed their ability to be digested by external proteases. Altogether they identified 83 unique proteins that were susceptible to
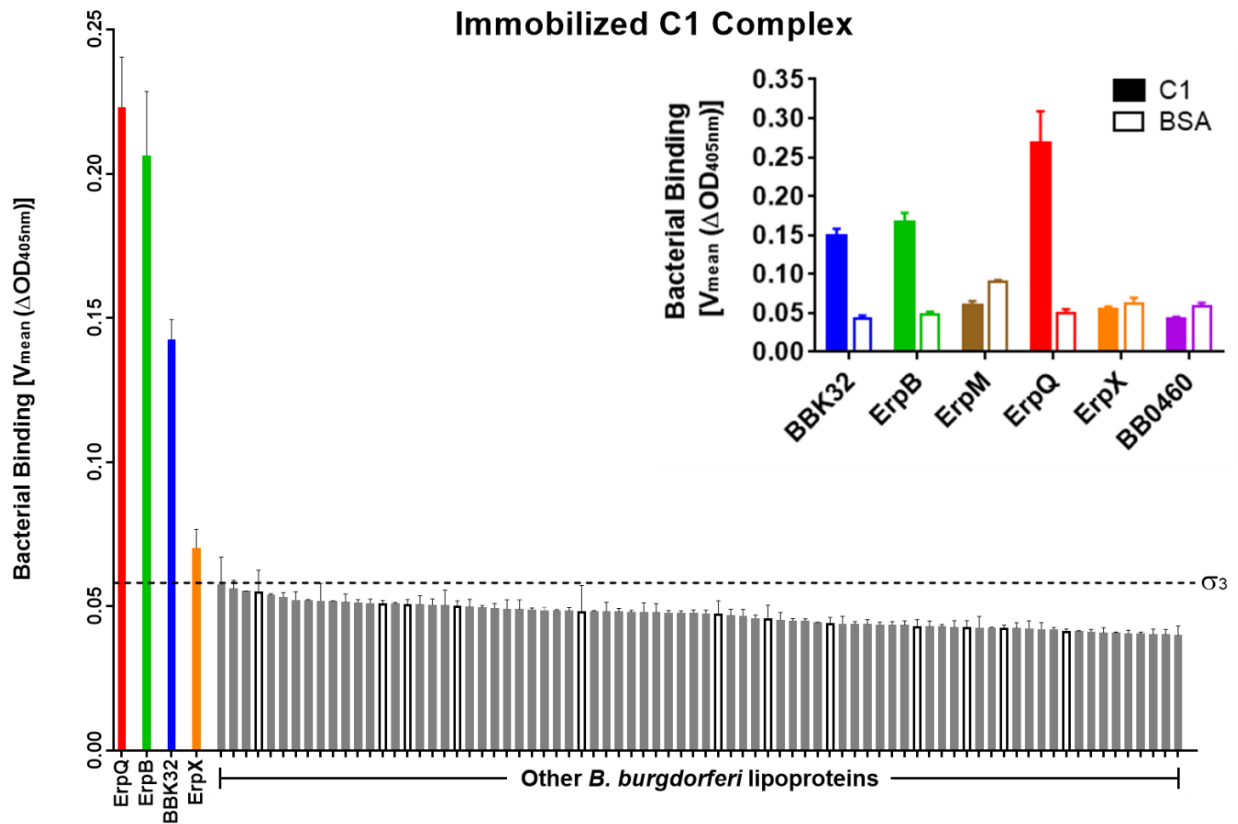
Figure 4. Gain of function spirochete library screen identifies C1 binding lipoproteins ErpB and ErpQ. 96-well plate coated with C1 Complex with each overexpression strain denoted by its lipoprotein. Bacterial binding was determined by Abs$_{405nm}$ over time with strains above 3 standard deviations (σ_3) over the mean intensity of the bottom 80% of strains that bind least efficiently colored. (**Inset**) Elp proteins in a separate binding assay to show specificity towards ErpB and ErpQ. BB0460 is a periplasmically expressed protein that was used as a control. BSA was used as a negative control to show background sensitivity and specificity. Figure adapted from Pereira, 2020[67].

protease degradation on the outer membrane. By studying surface exposed proteins, we can better characterize the interactions associated with the host pathogen axis.

In collaboration with the Zuckert Lab, Dr. Michael Pereira and Dr. Beau Wager, in Dr. Jon Leong's lab sought to find other proteins that interact with complement proteins as well as

many other relevant ligands[67]. Using an ELISA-based screen they found that two spirochete strains expressing ErpB and ErpQ bound C1-coated wells significantly more than spirochetes expressing other surface lipoproteins (**Fig. 4)**. This system also identified the known C1 interacting lipoprotein BBK32, as well as another paralog to ErpB/Q, ErpX, which was later found to not interact with C1 in a significant way (**Fig 4 inset**). This finding supports further interaction with the complement system that was previously unknown.

Given the collective insight of many years of research, *Borreliella* is emerging as a model organism for the study of complement evasion and employs many mechanisms to inhibit the innate immune response[43,44]. This study describes the novel mechanism of inhibition of complement protease C1s through interaction with a known exosite. Thus, contributing to our knowledge of CP evasion techniques by an important human pathogen, and providing insight into mechanisms of C1 activation.

CHAPTER 2: Materials and Methods

Plasmids constructed and oligonucleotides

All plasmid constructs and oligonucleotides are listed in **Table 1.** Propagation of

plasmids was performed in *E. coli* DH5α and protein expression was performed using

transformed *E. coli* BL21(DE3). Cells were cultivated using Terrific Broth (Fisher Scientific)

supplemented with 50 µg/mL kanamycin or 100 µg/mL carbenicillin, for pT7HMT or pGEX4T-

2 containing strains, respectively.

GST associated constructs pGEX4T-2, pMP17 and pMP18 containing *erpQ* and *erpB*

respectively, were provided by Dr. John Leong's lab and served as template DNA for all Erp

containing plasmids constructed in this study.

C1s constructs were constructed using native amino acid sequences P09871 (Uniprot)

with construct specific domain truncations. Domain truncations were *E. coli* optimized double

stranded DNA synthesized gBlocks (IDT) with flanking 5' BamHI and 3'NotI restriction sites

with a STOP codon. Subsequent digestion and insertion of DNA into pT7HMT was performed.

Erp oligonucleotides primers were designed with 5' BamHI and 3' NotI restriction

enzyme sites and 3' STOP site for insertion into pT7HMT. Due to a BamHI site in *erpB* the full-

length (ErpB 19-378) gene was designed with a 5' SalI site. PCR was completed with Q5 Master

mix (NEB) according to manufactures instructions with gradient PCR with from 60-70° C.

Subsequent ligation of product was performed with T4 DNA ligase (NEB) and sequence

validated using Simple Seq (Eurofins). All plasmids were transformed to appropriate strain using

chemically competent cells with incubation of 1 µL plasmid with 20 µL competent cells on ice

for 5 min. After incubation cells were quickly submerged into a 42° C dry bead bath for 90 sec

followed by a subsequent incubation on ice for 2 min. Transformed cells were then recovered using 300 µL LB Broth (Fisher Scientific) for 1 hr at 37° C and plated on LB agar with appropriately supplemented antibiotic.

Table 1. Primers and Constructs.

Construct Name	Vector	Primers	Ref.
pMP18 *erpB*	pGEX4T-2	-	Leong Lab
ErpB 19-378	pT7HMT	AAAAAAGTCGACAAGAATTATGCAATTAAAGA	This Study
		TTTTTTGCGGCCGCTTAATCTTCTTCATCATAATTAT	
ErpB 111-378	pT7HMT	AAAAAAGGATCCGCGGAACAAAGTGATGGTCAACAA	This Study
		TTTTTTGCGGCCGCTTAATCTTCTTCATCATAATTATCC	
ErpB 138-378	pT7HMT	AAAAAAGGATCCAAACAAGAGAATACAGAAGA	This Study
		TTTTTTGCGGCCGCTTAAATCTTCTTCATCATAATTATCCT	
ErpB 138-288	pT7HMT	AAAAAAGGATCCAAACAAGAGAATACAGAAGA	This Study
		TTTTTTGCGGCCGCTTAGTCGTTATCATCTTCCAAAT	
ErpB 182-378	pT7HMT	AAAAAAGGATCCCAAGAAAGAAAAGCTAAGGCAGA	This Study
		TTTTTTGCGGCCGCTTAAATCTTCTTCATCATAATTATCCT	
ErpB 243-378	pT7HMT	AAAAAAGGATCCATTGATGTTATAAAAGAGCA	This Study
		TTTTTTGCGGCCGCTTAATCTTCTTCATCATAATTATCC	
ErpB 288-378	pT7HMT	AAAAAAGGATCCGACGAAGGATTAGGAAAGCTATTA	This Study
		TTTTTTGCGGCCGCTTAATCTTCTTCATCATAATTATCC	
pMP17 *erpQ*	pGEX4T-2	-	Leong Lab
ErpQ 19-343	pT7HMT	AAAAAAGGATCCAAGAATTTTGCAACTGGTAA	This Study
		TTTTTTGCGGCCGCTTACTGACTGTCACTGATGTATC	
ErpQ 103-343	pT7HMT	AAAAAAGGATCCATAGAACAAAGTGATGGTCAAC	This Study
		TTTTTTGCGGCCGCTTATGCTTTTAATACTAATGCAT	
ErpQ 19-216	pT7HMT	AAAAAAGGATCCAAGAATTTTGCAACTGGTAA	This Study
		TTTTTTGCGGCCGCTTAATTTTCATTGATCTCATCTA	
ErpQ 168-343	pT7HMT	AAAAAAGGATCCCAGCAGCGTAAAGCTAAAGCTGA	This Study
		TTTTTTGCGGCCGCTTACTGACTGTCACTGATGTATC	
ErpQ 168-328	pT7HMT	AAAAAAGGATCCCAGCAGCGTAAAGCTAAAGCTGA	This Study
		AAAAAAGCGGCCGCTTAATCTTTAAGATATTTTTTAAC	
ErpQ 181-343	pT7HMT	AAAAAAGGATCCCGTGAAGAAGCTGAACAGCAGAAACGT	This Study
		TTTTTTGCGGCCGCTTACTGACTGTCACTGATGTATC	
ErpQ 217-343	pT7HMT	AAAAAAGGATCCATTGATGTTATAAAATGGCA	This Study
		TTTTTTGCGGCCGCTTACTGACTGTCACTGATGTATC	

Table 1. Primers and constructs cont.

Construct Name	Vector	Cloning Strategy	Ref.
C1r CCP2-SP	pT7HMT	-	Rushing et al[68]
C1s CCP2-SP	pT7HMT	Gene designed with gBlock	This Study
C1s CCP2-SP S632A	pT7HMT	Gene designed with gBlock	This Study
C1s CCP1-CCP2-SP	pT7HMT	Gene designed with gBlock	This Study
C1s CUB2-CCP1	pT7HMT	Gene designed with gBlock	This Study
C1s CUB2-CCP1-CCP2	pT7HMT	Gene designed with gBlock	This Study
C1s CCP1-CCP2-SP ABE	pT7HMT	Gene designed with gBlock	This Study
C1s CCP1-CCP2-SP Hinge	pT7HMT	Gene designed with gBlock	This Study
C1s CCP1-CCP2-SP ABE/Hinge	pT7HMT	Gene designed with gBlock	This Study

Protein Expression and Isolation

Following fresh transformation into *E. coli* BL21(DE3), cells were grown overnight in 10 mL of Terrific Broth supplemented with 100 µg/mL kanamycin. The next day the cells were inoculated into 1L of Terrific Broth supplemented with 100 µg/mL kanamycin at 37° C and monitored to an OD_{600} between 0.6 - 0.8. Cells were then induced with 1 mM Isopropyl β- d-1-thiogalactopyranoside (IPTG) and transferred to 16° C overnight. Cells were then centrifuged at 6,000 RPM and resuspended in 100 mL Ni-NTA-binding buffer (20 mM Tris (pH 8.0), 500 mM NaCl, 10 mM Imidazole (pH 8.0)) and lysed through microfluidization with an LM-10 Microfluidizer (Microfluidics). Crude lysate was then centrifuged again at 25,000x g and supernatant flowed over a gravity-flow column with His resin (Gold Bio). After washing the resin with 25 mL Ni-NTA-binding buffer protein was slowly eluted with 15 mL Ni-NTA-elution buffer (20 mM Tris (pH 8.0), 500 mM NaCl, 500 mM imidazole (pH 8.0)) and exchanged back into Ni-NTA-binding buffer using a Hi-prep Desalting 26/10 column (GE Healthcare) on an

AKTA pure (GE Healthcare). Removal of His-myc affinity tag then followed with incubation of 50 µg tobacco etch virus (TEV) protease and 5mM β-mercaptoethanol at room temperature overnight. Digested proteins were then isolated from their tag by collecting their flow through on a 5mL HisTrap-FF column (GE Healthcare). Further isolation of the proteins by size exclusion chromatography was performed using a HiLoad 26/600 Superdex 75pg column equilibrated to HBS (10 mM HEPES pH 7.3, 140 mM NaCl). Monodisperse peaks were collected and analyzed by SDS-PAGE for purity and stored at -80° C until use.

Constructs in pGEX4T-2 were expressed and isolated according to manufacturer's instructions (GE Healthcare) with no further isolation.

Recombinant C1r CCP2-SP was expressed and isolated as previously described[68]. C1s constructs (**Table 1**) were similarly expressed and isolated with the following modifications. C1s is produced as a zymogen and is not capable of autoactivating. Activation of C1s proenzyme constructs was performed by incubation with 25 nM C1r enzyme (Comp Tech) overnight at 37° C and subjected to analytical gel filtration with a Superdex 200 Increase 10/300 GL (GE Healthcare). The smaller of 2 monodisperse peaks was collected, analyzed by SDS-PAGE, and utilized for binding experiments.

Surface plasmon resonance

Binding of C1 and its sub-components to GST-ErpB and GST-ErpQ was performed at 25°C using a Biacore T200 (GE Healthcare) as previously described[50,51], with the following modifications. GST-ErpB and GST-ErpQ were amine coupled to the CMD200 (Xantec bioanalytics) at 10 µg/ml in 10 mM sodium acetate pH 4.0 or 10 mM sodium acetate pH 3.5 for $ErpQ_{181-343}$ and $ErpB_{182-378}$. Final immobilization densities shown in resonance units (RU) are presented in **Table 2**. HBS-T $Ca2^+$ (10 mM HEPES (pH 7.3), 140 mM NaCl, 0.005% (v/v)

Tween 20, 5 mM CaCl$_2$) was used as the running buffer and a flowrate of 30 μl min^{-1} was used in all experiments. All analytes were buffer exchanged into running buffer prior to experimentation.

C1 complex (Complement Technologies) was injected over ligands in a two-fold concentration series: .59, 1.2, 2.3, 4.7, 9.4, 18.8, 37.5, 75, and 150 nM for 120 sec, followed by 180 sec dissociation. The surface was then regenerated by injecting 2 M NaCl for 60 sec 3 times consecutively, bringing the response to baseline. The same approach was used for proenzyme C1r, C1r enzyme, proenzyme C1s, and C1s enzyme (Complement Technologies). A separate ranking experiment was completed on the same surface with C1 components C1, C1q, C1r enzyme, and C1s enzyme at 150 nM.

Recombinant activated enzymes and truncations were similarly analyzed, using a two-fold concentration series of 0.39, 0.78, 1.6, 3.1, 6.3, 13, 25, 50, 100, and 200 nM. Steady state analyses were performed on each sensorgram series using the Biacore T200 Evaluation Software 3.1 (GE Healthcare) and a 1:1 (Langmuir) binding model. All SPR experiments were completed in triplicate.

Table 2. SPR Immobilization Densities

Ligand	Immobilization Density (RU)	Figures Surface was Used
GST-ErpQ	451.1	**Figure 5 and 6**
GST-ErpB	555.1	**Figure 5 and 6**
GST-ErpQ	495.8	**Figure 7**
GST-ErpB	537.9	**Figure 7**
ErpQ 19-343	986.3	**Figure 14**
ErpQ 168-343	473.1	**Figure 14**
ErpB 138-378	449.5	**Figure 14**
ErpQ$_{19-343}$	206	**Figure 16**
ErpQ$_{181-343}$	311	**Figure 16**
ErpB$_{182-378}$	574.7	**Figure 16**

Inhibition of C4b deposition by recombinant B. burgdorferi lipoproteins

Direct inhibition of classical pathway activation was assessed by ELISA. Three µg/ml of classical pathway activator Human IgM (Innovative Research) in 100 mM Na_2CO_3/$NaHCO_3$ coating buffer, pH 9.6, was immobilized overnight at room temperature in high-binding polypropylene microplates (Grenier bio-one). Between each step described below plates were washed 3X with 100 µl/well of TBS-T (50mM Tris (pH 8.0),150 mM NaCl, 0.05% (v/v) TritonX-100). Unbound regions of the plate were then blocked with PBS-T-BSA (137mM NaCl, 2.7 mM KCl, 10mM Na_2HPO_4,1.8 mM KH_2PO_4, 1%(w/v) bovine serum albumin, and 0.05% (v/v) Tween-20) for 1 hour at 37°C. Classical pathway-mediated complement activation was then induced by adding 2% final pooled Normal Human Serum (Innovative Research) in a two-fold dilution series of each inhibitor of interest in CP Buffer (10 mM HEPES (pH 7.3), 0.1%

(w/v) gelatin type A, 140 mM NaCl, 2 mM CaCl$_2$, 0.5 mM MgCl$_2$), and incubated at 37°C for 1 hour. A 1:300 dilution anti-C4 antibody (HYB 162-02) (Santa Cruz Biotechnology) in CP Buffer was then added, and plates were incubated at 37°C for 1 hour. A 1:3000 dilution of goat anti-mouse HRP secondary antibody (Thermo Scientific) was then added at room temperature with light rocking for 1 hour. Activation of HRP conjugated antibody was detected at room temperature using 1-step Ultra TMB ELISA (Thermo Scientific) for 10 min with rocking in the dark. The reaction was stopped by adding .16 N sulfuric acid, and the absorbance was measured at 450 nM on an EnSight multimode plate reader (PerkinElmer). Data were in-column normalized using cells containing serum only, or buffer with no serum, as 100% and 0% signal, respectively. All experiments were performed in triplicate and IC50 values were determined using a variable four-parameter nonlinear regression analysis using GraphPad Prism 8.1.2.

Inhibition of C1r CCP2-SP and C1s enzyme activity by synthetic peptide cleavage

C1r CCP2-SP enzyme and C1s enzyme assays were performed in HBS-Ca2$^+$ (10 mM HEPES (pH 7.3), 140 mM NaCl, 5 mM CaCl2). 25 µM BBK32-C or GST-ErpQ were incubated with final concentrations of 1.5 nM C1r CCP2-SP or 5 nM C1s enzyme for 10 min at room temperature. C1r CCP2-SP enzyme assays were performed with the addition of 300 µM Z-Gly-Arg-Thiobenzyl Ester (MP Biomedical) and 100 µM 5,5′-dithiobis(2-nitrobenzoic acid) (DTNB) (TCI) just prior to measurement[68,69]. C1s enzyme assays were performed with the addition of 100 µM Z-L-Lys Thiobenzyl Ester HCl (Sigma) and 100 µM DTNB just prior to measurement[70]. Final reaction volumes were 80 µL for both assays. Abs$_{412}$ measurements were conducted on an EnSight multimode plate reader (PerkinElmer) after 1 hour both C1r enzyme assay and C1s enzyme assays at 25° C. Data were in-column normalized by including the C1s enzyme or C1r enzyme with respective substrate as 100% activation, and no enzyme as 0% activation.

C1r enzyme cleavage inhibition of proenzyme C1s

Inhibition of C1r enzyme cleavage of proenzyme C1s was assayed by incubation of 1 µM C1r enzyme with 1 µg of proenzyme C1s with a 2-fold curve of inhibitor in HBS-Ca2+ in a final volume of 10 µL. The reaction was then incubated at 37° C for 1 hr and was stopped by addition of 5µL reducing SDS-PAGE loading buffer (150 mM Tris pH 7.0, 12% Sodium dodecyl sulfate (SDS), 6% β-mercaptoethanol, 30% glycerol, 0.05% bromophenol blue). Cleavage of proenzyme C1s was determined by 10% SDS-PAGE analysis with BBK32-C used as a control for inhibition.

C1s enzyme cleavage inhibition of natural substrates C2 and C4 by Erp proteins

Inhibition of C1s enzyme direct cleavage was assayed by incubation of 6.25 nM C1s enzyme with a twofold curve of inhibitor and 1.25 µL C2 (.5 mg/mL) or 1.25 µL C4 (1 mg/mL) in HBS-Ca2$^+$ for a final volume of 10 µL. The reaction was then incubated at 37° C for 1 hr and was stopped by addition of 5µL reducing SDS-PAGE loading buffer (150 mM Tris pH 7.0, 12% Sodium dodecyl sulfate (SDS), 6% β-mercaptoethanol, 30% glycerol, 0.05% bromophenol blue). Cleavage of substrates was determined by 10% SDS-PAGE analysis and subsequent densitometry with Image Lab (Bio-Rad). C2 cleavage was determined by formation of the C2b band by normalizing to an enzyme C2 control 100% and non-enzyme treated C2 at 37° C. C4 was in lane controlled via densitometric analysis of the common C4β which migrates at ~70kDa. The development of the C4α' chain was monitored by taking the ratio of C4α' over the sum of C4α, C4α' and C4β. IC50's for both substrates were determined using a normalized four-parameter curve.

Amplified luminescence homogenous proximity assay

Amplified luminescence homogenous proximity assay (ALPHA) were performed according to manufactures recommendations with the following modifications. Direct ALPHA experiments were performed with 12.5 nM GST-ErpQ and 150 nM His-C1r-CCP2-SP in the presence of 20 µg/mL GST-Donor beads and 20 µg/mL His-Acceptor beads. Indirect ALPHAs were performed with 12.5 nM GST-ErpQ and 150 nM His-BBK32-C in the presence of 20 µg/mL GST-Donor beads and 20 µg/mL His-Acceptor beads. All experiments were carried out with the addition of a twofold concentration curve of non-tagged species to assess competition or simultaneous binding. Reactions were carried out in HBS-T Ca^{2+} in 25 µL total volume in 96-well ½Area ALPHAplates^{TM} (Perkin-Elmer) and incubated in the dark for 1 hr at room temperature. ALPHA signal was collected using an EnSight plate reader (Perkin-Elmer) with an excitement of 680 nm for 40 ms and emission accumulated for 130 ms. K_D's were approximated using the Cheng-Prussoff equation and determined using a normalized four-parameter curve in GraphPad 8.0 (Prism)[71].

CHAPTER 3: ErpB and ErpQ Bind to C1 Complex Proteases C1r and C1s and Potently Inhibit the Classical Pathway of Complement

ErpB and ErpQ specifically bind to C1 proteases

Screening of the gain-of-function expression library against various ligands, including complement components, by the Leong lab showed that expression of borrelial lipoproteins ErpB and ErpQ resulted in enhanced binding to C1 complex (**Fig 4**). To better describe these interactions, GST-ErpB and GST-ErpQ was covalently immobilized on a biosensor chip and analyzed for interactions with C1 complex as an analyte by surface plasmon resonance (SPR) (**Appendix A**). In agreement with the gain of function data collected by the Leong Lab (**Fig 4**), recombinant GST-ErpB and GST-ErpQ both bound C1 with high affinity (**Fig 5A**).
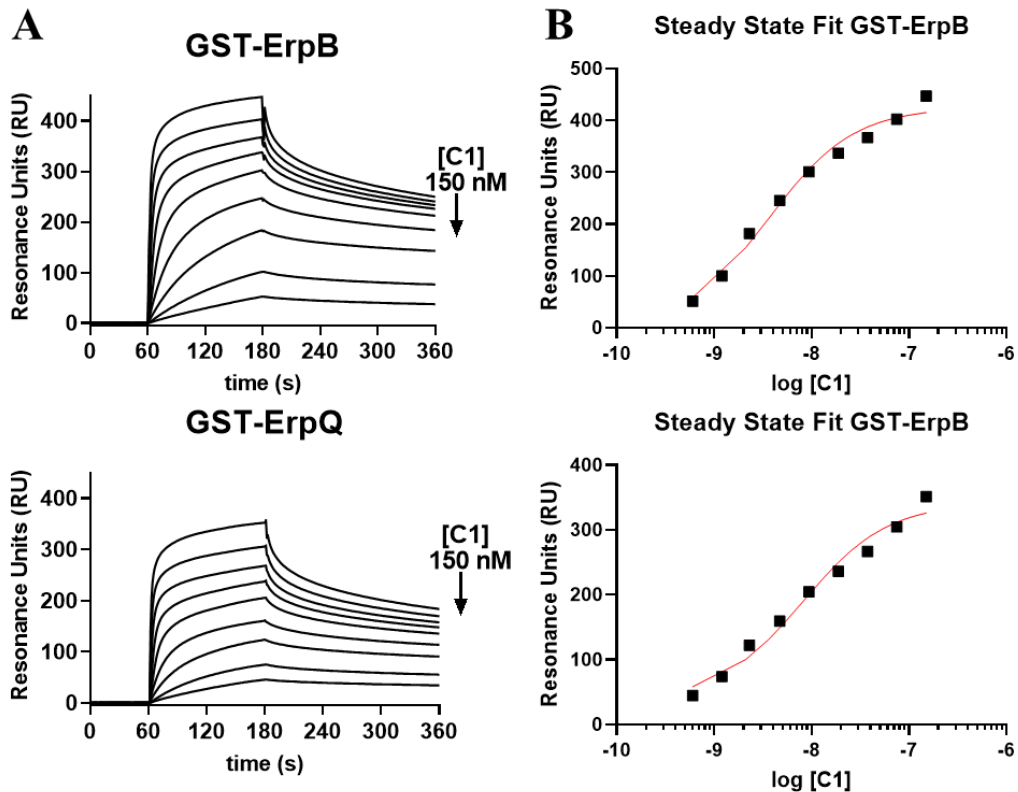
Figure 5. Recombinant GST-ErpB and GST-ErpQ form high affinity interactions with C1 complex. A) Multi cycle SPR sensorgrams of a two-fold dilution series of C1 complex (0.6-150 nM) over GST-ErpB or GST-ErpQ. Top curve represents 150 nM C1 injection with HBS-T Ca^{2+} running buffer. **B)** Steady state fits of adjacent multi cycle curves with RU at steady state (black squares) and steady state fits (red line). Sensorgrams and fits are a shown as a representative set with all experimentation performed in triplicate.

Steady state fits of these data reveal similar high affinity binding of recombinant GST-ErpB ($K_{D,SS}$ = 5.6 nM) and GST-ErpQ ($K_{D,SS}$ = 11 nM) to C1 (**Fig 5B, Table 3**).

The C1 complex is made up of three subcomponents: i) the pattern recognition molecule C1q is a large collagen-like hexameric protein with six globular domains, which is bound to the heterotetrametric serine proteases of C1, C1r$_2$s$_2$, ii) the initiating protease of the CP, C1r, exists as a zymogen heterotetramer with its substrate iii) protease C1s (**Fig 6A**). To determine what subcomponent the Erps were interacting with, I employed a surface plasmon resonance (SPR) based ranking study in which each subcomponent is used as an analyte assaying for their ability to bind covalently surface bound Erp. Single injections of 150 nM were employed using C1 complex (C1qr$_2$s$_2$), C1r, C1s, and C1q over GST-ErpB and GST-ErpQ. Based on increase in RU

Figure 6. GST-ErpB/Q bind to C1 complex with high affinity. A) Cartoon model of C1 complex C1q (green), $C1r_2$ (red) and $C1s_2$ (cyan). **B)** Analysis of SPR ranking study to determine specificity of GST-Erp constructs for C1 subcomponents. C1 complex components were 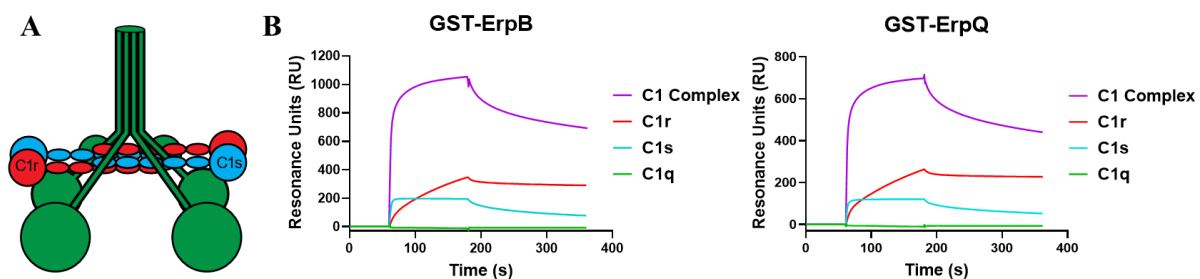injected at 150 nM in HBS-T Ca^{2+} individually over surface immobilized GST-ErpB or GST-ErpQ. Injections of the full C1 complex, protease C1r, and protease C1s promoted binding whereas C1q did not produce significant binding. Sensorgrams are representative sample of experimentation in performed in triplicate.

and subsequent slow off rate the data show that ErpB/Q interact with C1 complex serine protease components C1r and C1s, but not C1q (**Fig 6**). Altogether the data presented support that ErpB and ErpQ form high affinity interactions with the C1 complex through binding of the serine proteases C1r and C1s.

Functionally C1 complex exists as a zymogen, which upon recognition of immune complexes on activating surfaces becomes enzymatically competent. This activation is induced by dramatic conformational changes in each of the components of C1, including the proteases. The activation of the proteases allows them to perform their catalytic functions and induces differential surfaces for the recognition of their substrates (**Appendix B**)[72–74]. Due to these apparent differences we wanted to know if conformational changes were important in the recognition of ErpB and ErpQ. Using an SPR-based approach we immobilized GST-Erp proteins and injected a series of zymogen and active C1r and C1s. Interestingly the ligands were able to distinguish between the activation states of both C1r and C1s, with both Erp proteins preferentially binding to the activated enzymes over the proenzyme forms (**Fig 7**). These experiments revealed that there was a ~68-fold difference in affinity of C1s enzyme recognition
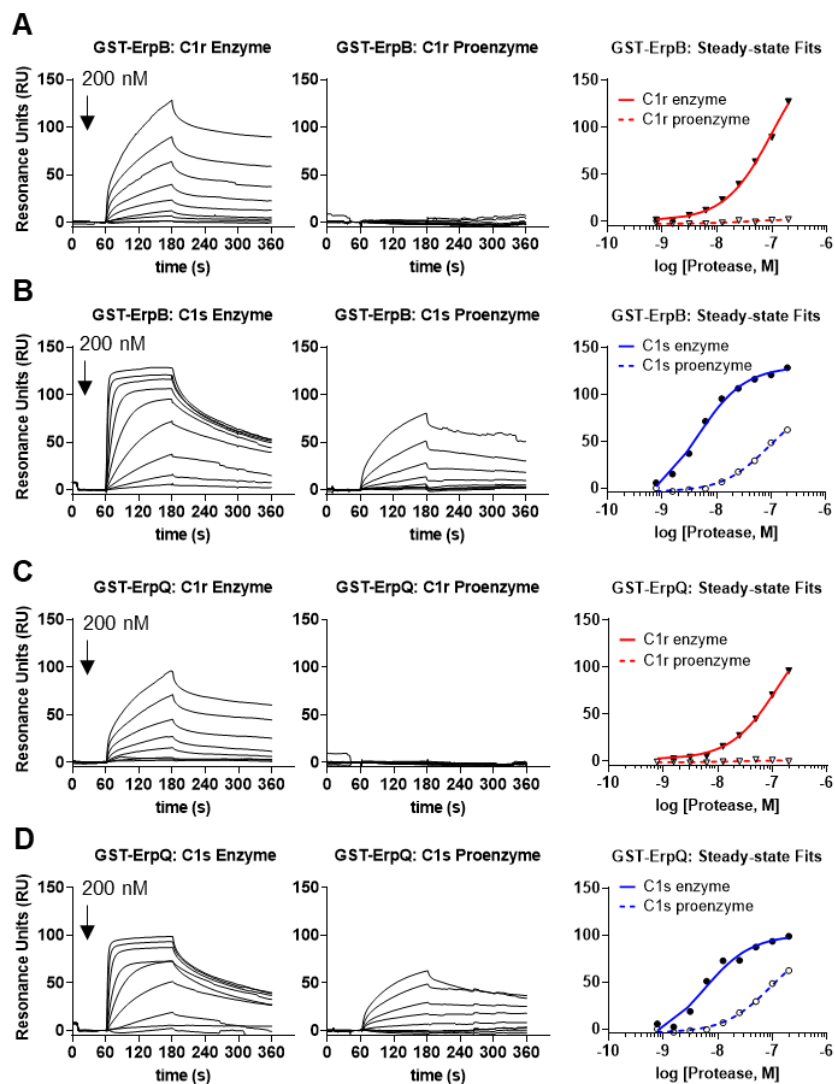
Figure 7. GST-ErpB/Q preferentially bind to active C1r and C1s over proenzyme C1r and C1s. SPR analysis of enzymatic conformational sensitivity was used to determine preference in binding of GST-ErpB (**A-B**) and GST-ErpQ (**C-D**). A twofold series of injections were performed (200-0.8 nM) with each form of C1r (**A, C**) or C1s (**B, C**) in HBST-Ca^{2+}. Enzyme forms bound with higher affinity as shown in steady state fits in the third panels (**A-D**). All forms of C1r and C1s bound, except C1r proenzyme. All experiments were performed in triplicate.

over its proenzyme form in GST-ErpB and a ~38-fold difference in GST-ErpQ binding (**Table 3**). C1r recognition was even more impeded by the proenzyme conformation with little to no

binding for proenzyme (**Fig 7A, C**). Furthermore, we determined the steady state affinities of the

proteases and found that GST-ErpB preferentially bound C1s enzyme ($K_{D,SS} = 3.9$ nM) over C1r

enzyme ($K_{D,SS} = 100$ nM) a ~25-fold change in affinity. This was consistent with values obtained

for GST-ErpQ with C1s enzyme ($K_{D,SS} = 97$ nM) over C1r enzyme ($K_{D,SS} = 4.5$ nM) a ~22-fold

change in affinity (**Table 3**). These data support high affinity binding of enzymatically active

forms of C1 protease components C1r and C1s over their proenzyme forms to ErpB and ErpQ

and emphasize the importance of conformational dynamics in protein interaction.

Table 3. Steady State Affinities for ErpB and ErpQ Analytes

Ligand	Analyte	$K_{D,SS}$ (nM)	Ligand	Analyte	$K_{D,SS}$ (nM)
GST-ErpQ	C1 Complex	11 ± 2.0	GST-ErpB	C1 Complex	5.6 ± 1.5
	C1s Enzyme	4.5 ± 0.84		C1s Enzyme	3.9 ± 0.40
	C1r Enzyme	130 ± 29		C1r Enzyme	100 ± 22
	C1s Proenzyme	168 ± 60		C1s Proenzyme	270 ± 45
	C1r Proenzyme	n.d.		C1r Proenzyme	n.d.
ErpQ$_{19-343}$	C1s CCP1-CCP2-SP WT	150 ± 0.5	ErpQ $_{182-378}$	C1s CCP1-CCP2-SP WT	360 ± 16
	C1s CCP1-CCP2-SP Hinge	320 ± 12		C1s CCP1-CCP2-SP Hinge	574 ± 110
	C1s CCP1-CCP2-SP ABE	n.d.		C1s CCP1-CCP2-SP ABE	n.d.
	C1s CCP1-CCP2-SP Hinge/ABE	n.d.		C1s CCP1-CCP2-SP Hinge/ABE	n.d.
ErpQ $_{181-343}$	C1s CCP1-CCP2-SP WT	210 ± 0.5			
	C1s CCP1-CCP2-SP Hinge	370 ± 0.5			
	C1s CCP1-CCP2-SP ABE	n.d.			
	C1s CCP1-CCP2-SP Hinge/ABE	n.d.			

ErpB and ErpQ are inhibitors of the Classical Pathway

After learning of their high affinity interactions with the classical pathway proteases we were interested in determining if ErpQ and ErpB could inhibit the C1 complex at the level of C4 deposition. To determine the function of these proteins an ELISA-based complement assay was used, which takes advantage of the covalent nature of C4 deposition by CP activation. Using a potent borrelial inhibitor known to inhibit the classical pathway, BBK32-C, as a control we found that GST-ErpB and GST-ErpQ both inhibit the classical pathway at the level of the C1 complex (**Fig 8A**). Though not nearly as potent as BBK32-C (18 nM), GST-ErpB (330 nM) and GST-ErpQ (260 nM) both specifically and efficiently classical pathway activation.

Next, we were interested in whether the expression of these proteins on *B. burgdorferi* B31e-2 imparted protection from CP-mediated cell lysis. The Leong Lab assayed for the ability of ErpB and ErpQ to confer protection to serum killing under classical pathway activation in a B31e-2 background. Using *Borrelia* B31 specific antibodies they were able to effectively activate the classical pathway initiating the killing of CP sensitive spirochetes. Only spirochetes expressing BBK32, ErpB or ErpQ were able to deter CP-mediated killing whereas periplasmically expressed BB0460 was killed relative to an isotype control, which was not specific for *Borrelia* and therefore did not activate the CP (**Fig 8B**).
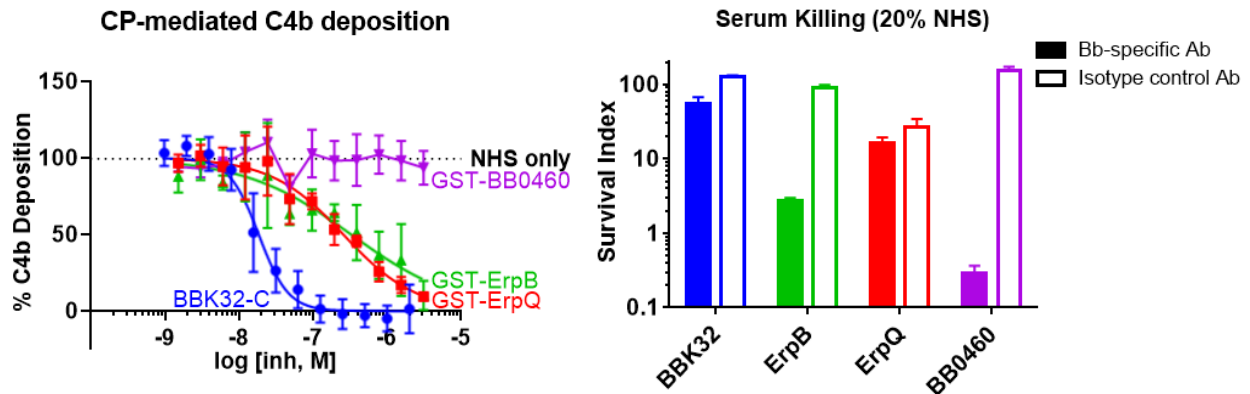
Figure 8. ErpB and ErpQ are inhibitors of the classical pathway activation and promote serum survival of *B. burgdorferi*. A) Dose dependent classical pathway inhibition was assayed by selectively activating the CP through immobilized IgM. Two-fold dilutions of inhibitor were incubated with 2% normal human sera in CP buffer. A monoclonal antibody against C4d was used to determine C4b deposition amount. Data were completed in triplicate and normalized to sera only and no sera controls. **B)** Classical pathway sensitivity was determined through activation of the classical pathway by a *Borrelia* specific antibody. Only spirochetes expressing classical pathway inhibitors were able to deter killing compared to nonspecific isotype control. In both experiments BBK32-C and GST-BB0460 were included as positive and negative controls of CP inhibition, respectively. Data in **B** completed by Dr. Michael Pereira (*unpublished data*).

Collectively the data presented depict functional cause and effect of expression of ErpB and ErpQ to confer protection against classical pathway mediated killing. With an ascribed function of classical pathway inhibition elucidated we sought to understand the molecular mechanisms of this interaction. This led us to determining the functional domain on ErpB and ErpQ that fully contributes to its complement inhibitory abilities. To achieve this, I truncated ErpB and ErpQ in a successive manner where the C4b deposition ELISA was utilized to screen for residual complement inhibitory function. Successful expression of native full length untagged ErpQ (ErpQ$_{19-343}$) allowed for analysis of truncations without effects that a tag such as GST or

His may be able to contribute. First, I selected a region in the C-terminus denoted $ErpQ_{103-343}$ in addition to a pair of complementing N- and C- terminal constructs, $ErpQ_{19-216}$ and $ErpQ_{217-343}$, respectively (**Fig 9**). However, only the longer C-terminal $ErpQ_{103-343}$ conferred $ErpQ_{19-343}$-like inhibition, which led to the construction of several more constructs assaying the N-terminal amino acids of each construct between 103 and 217. This led to the creation of $ErpQ_{181-343}$, which conveyed full CP inhibitory capacity. Interestingly, when a similar construct $ErpQ_{168-343}$ was truncated by only 15 amino acids from the C-terminus there was a ~6-fold difference in IC_{50} (**Table 4**). Using this approach, I implemented a similar series of truncations (**Fig 9**).

Figure 9. Identification of C-terminal complement inhibitory domain of ErpQ. A) Graphical representation of ErpQ constructs presented in (**B**) by length of bar. Constructs that inhibited C4b deposition similarly to the full-length molecule (green), intermediate difference in inhibitory ability (yellow), and not detectable inhibition (red). **B**) Classical pathway inhibition of ErpQ truncations was assayed by C4b deposition with 2% normal human sera in the presence of immobilized IgM. Dose dependent inhibition of CP by ErpQ truncations was determined with a twofold concentration series performed between one and three times.

on ErpB to identify its complement inhibitory domain. Unfortunately, expression and isolation of $ErpB_{19-378}$ was not achieved as protein yields from this construct were not of sufficient quantity

to validate similarity or difference from GST-ErpB. However, The C-terminal construct $ErpB_{111-378}$ effectively and potently inhibited CP mediated deposition of C4b in the ELISA assay similarly to the GST-ErpB (**Fig 10**). Further narrowing of the inhibitory domain from both
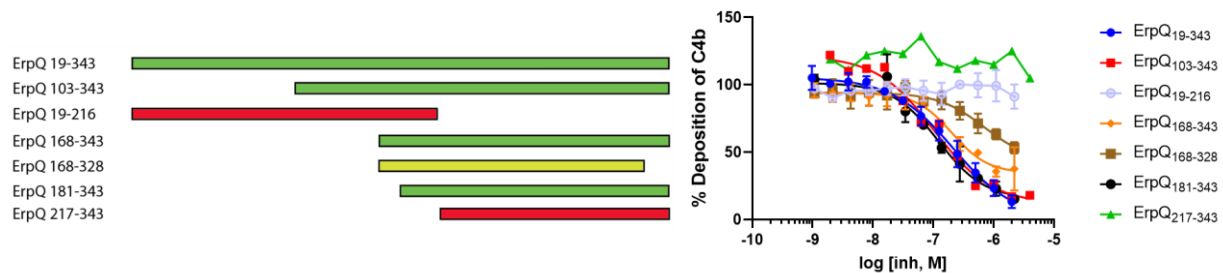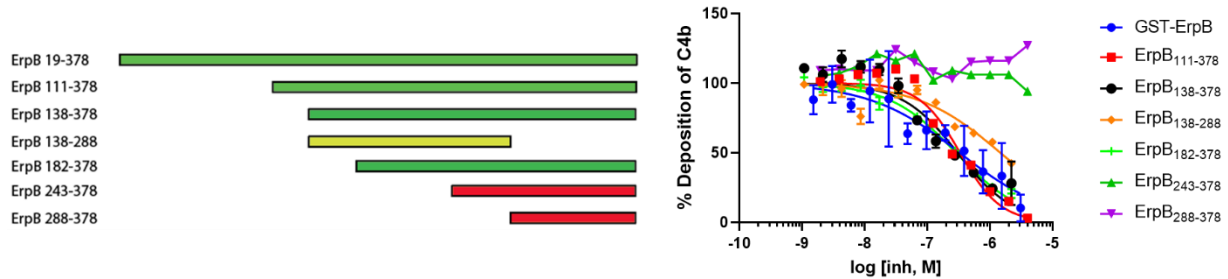

Figure 10. Identification of C-terminal complement inhibitory domain of ErpB. A) Graphical representation of ErpQ constructs presented in (**B**) by length of bar. Constructs that inhibited C4b deposition similarly to the full-length molecule (green), intermediate difference in inhibitory ability (yellow), and not detectable inhibition (red). **B)** Classical pathway inhibition of ErpQ truncations was assayed by C4b deposition with 2% normal human sera in the presence of immobilized IgM. Dose dependent inhibition of CP by ErpB truncations was determined with a twofold concentration series performed between one and three times.

the N- and C-terminus resulted in a similar pattern to that of ErpQ truncations with portions of the C-terminus contributing to inhibition and the N-terminal half not conveying complement inhibitory capability. The truncations used led to the discovery of the complete inhibitory domain $ErpB_{181-378}$. Taken together this implicates the importance of the C-terminal half of ErpB and ErpQ in and their importance for complement inhibitory function in the context of the full-length proteins.

Table 4. CP ELISA IC50 Data

Protein	IC$_{50}$ (nM)	95% C.I. (nM)	Protein	IC$_{50}$ (nM)	95% C.I. (nM)
GST-ErpQ	260	190 - 340	GST-ErpB	330	200 - 570
ErpQ$_{19-343}$	220	150 - 450	ErpB$_{111-378}$	330	240 - 480
ErpQ$_{103-343}$	100	53 - 200	ErpB$_{243-378}$	n.d.	n.d.
ErpQ$_{217-343}$	n.d.	n.d.	ErpB$_{288-378}$	n.d.	n.d.
ErpQ$_{263-343}$	n.d.	n.d.	ErpB$_{138-288}$	1500	1100 - 2300
ErpQ$_{168-343}$	200	150 to 340	ErpB$_{138-378}$	300	220 - 430
ErpQ$_{181-343}$	120	85 to 200	ErpB$_{182-378}$	290	250 - 330
ErpQ$_{168-328}$	700	305 to 1600	BBK32-C	18	15 - 23
ErpQ$_{19-216}$	n.d.	n.d.			

ErpB and ErpQ inhibit C1s through a novel mechanism

With the identification of the inhibitory domain, we were then interested in determining

the mechanism of CP inhibition. The most probable hypothesis was the ability of ErpB and ErpQ

to inhibit CP enzymes from cleavage of their natural substrates. This broke down the inhibition

into two steps: i) C1r cleavage of its natural substrate C1s proenzyme and ii) C1s cleavage of its

natural substrate C4. Testing this hypothesis involved the use of a gel-based technique which

takes advantage of the formation of differential products formed in the cleavage of scissile loops

on the substrates. These experiments were performed with $ErpQ_{19-343}$ to monitor full activity of

the inhibitor without the tag. First $ErpQ_{19-343}$ was incubated with C1r enzyme and C1s proenzyme

for an hour at 37° C. Despite high affinity interaction with C1r enzyme, $ErpQ_{19-343}$ exhibited no

inhibition of C1r mediated cleavage of C1s proenzyme (**Fig 11**). Alternatively, incubation of

$ErpQ_{19-343}$ with C1s enzyme and its natural substrate C4 yielded a complete inhibitory curve with
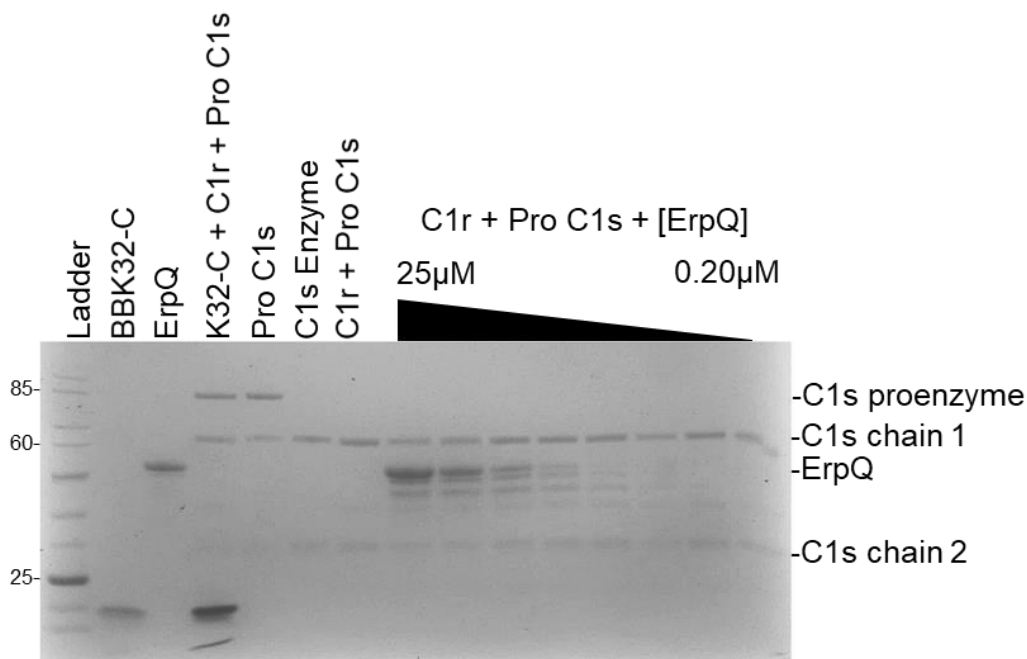
Figure 11. ErpQ$_{19-343}$ is not an inhibitor of C1r enzyme cleavage of C1s proenzyme. To determine if ErpQ$_{19-343}$ was able to inhibit C1r mediated cleavage of C1s proenzymes we employed SDS-PAGE analysis of substrate products in the presence of inhibitors. A twofold dose of ErpQ$_{19-343}$ was performed in the presence of C1r enzyme and C1s proenzyme. In each lane labelled above the gel only controls containing only C1s proenzyme, denoted Pro C1s, or BBK32-C, a potent C1r inhibitor, were capable of inhibiting formation of C1s enzyme chain 1. This is a representative gel and was performed in triplicated.

an IC$_{50}$ of ~10 µM (**Fig 12A and 12B**). This positive result then led us to assay for the inhibition of the downstream C1s enzyme substrate component C2. Inhibition of C2 cleavage was markedly more effective with an IC$_{50}$ ~1.4 µM (**Fig 12C and 12D**). This represents the first microbial inhibitor of the classical pathway complement protease C1s and furthermore is the first biologically derived C1s inhibitor shown to block C2 cleavage. Further validation of the complement inhibitory domain truncations of ErpB and ErpQ in this assay showed that both were able to block C1s enzyme mediated C2 cleavage in this assay (**Fig 13**). Here we do note a
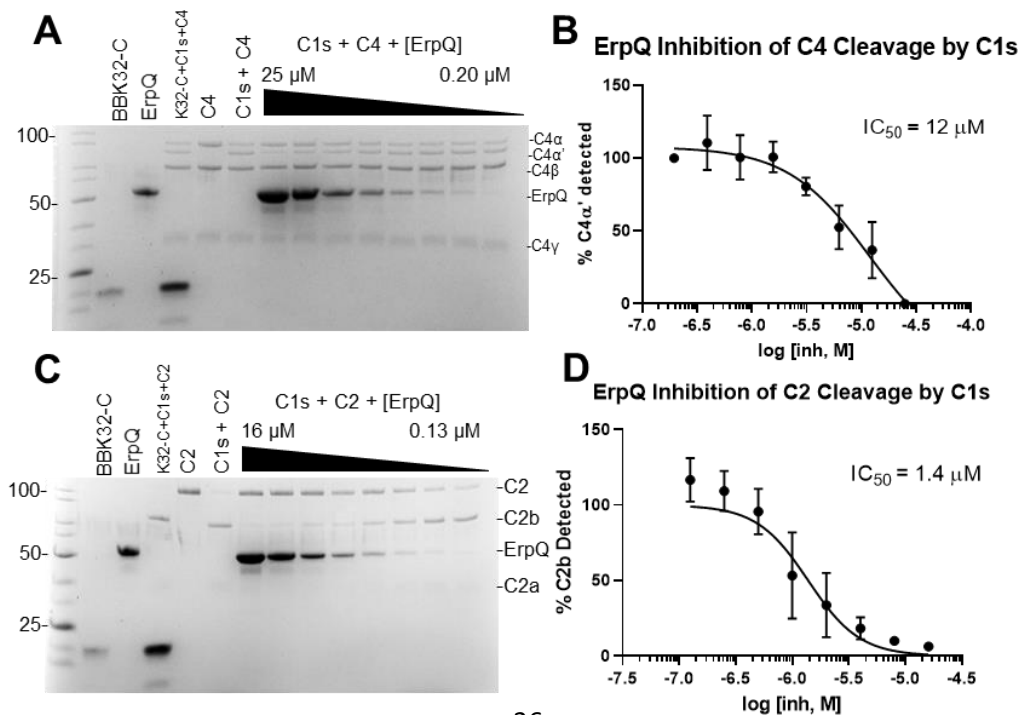
Figure 12. ErpQ$_{19\text{-}343}$ is a potent inhibitor of C1s mediated cleavage of natural substrates C4 and C2. Determination of C1s substrate cleavage inhibition by ErpQ$_{19\text{-}343}$ was performed by SDS-PAGE analysis. SDS-PAGE gels, contents denoted above each, of twofold dose curves with ErpQ$_{19\text{-}343}$ in the presence of 6.25 nM C1s enzyme and substrates 2.5 µg C4 (**A**) or 1.25 µg C2 (**B**) for 1 hour at 37° C. ErpQ$_{19\text{-}343}$ was able to inhibit band formation of C4α' (**A**) and C2b (**B**), whereas BBK32-C was unable to inhibit C1s enzyme. Densitometric analysis of band intensity was performed on the formation of C4α' (**A**) and C2b (**B**) in panels (**C**) and (**D**), respectively. IC$_{50}$ values reported are an average of three independent gels.

modest ~3-fold difference in inhibition by ErpQ$_{181\text{-}343}$ (IC$_{50}$ ~300 nM) over ErpB$_{182\text{-}378}$ (IC$_{50}$ ~800 nM). Collectively these data support the previous findings of CP inhibition through binding of C1s enzyme and potently inhibit deposition of C4, and subsequent inhibition of C2 cleavage, through a mechanism isolated to the C-terminus.
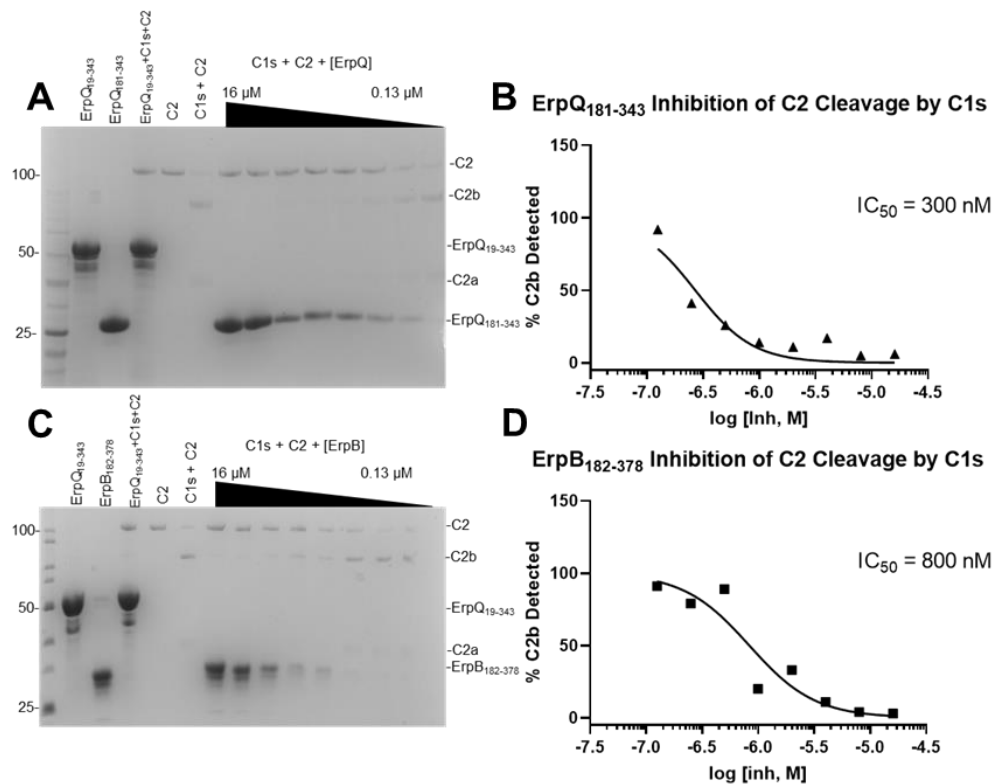
Figure 13. Complement inhibitory fragments ErpQ$_{181-343}$ and ErpB$_{182-378}$ maintain inhibition of C1s mediated cleavage of C2. Determination of C1s substrate cleavage inhibition by ErpQ$_{181-343}$ and ErpB$_{182-343}$ was performed by SDS-PAGE analysis. (**A, C**) SDS-PAGE gels of twofold dose curves with each inhibitor in the presence of 6.25 nM C1s enzyme and substrates 1.25 µg C2 for 1 hour at 37° C. ErpQ$_{181-343}$ and ErpB$_{182-343}$ were able to inhibit band formation of C2b (**A, C**), ErpQ$_{19-343}$ was used as a positive control for inhibition. Densitometric analysis of band intensity was performed on the formation C2b (**A, C**) in panels (**B**) and (**D**), respectively. IC$_{50}$ values reported are of a single experiment.
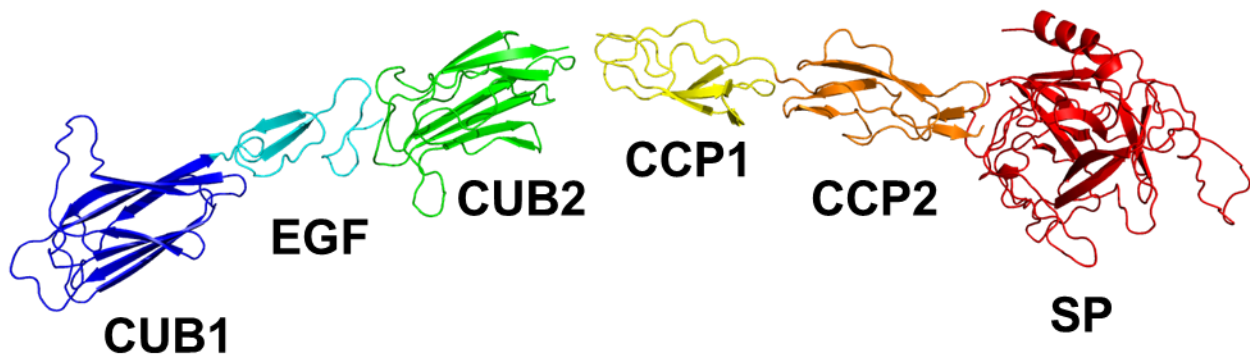
Figure 14. Model of full length C1s. Cartoon model of full length C1s (SASDB: SASDBZ7). Each domain is labelled underneath with colors distinguishing segments of the molecule. Abbreviations: CUB, complement <u>C</u>1r/C1s – <u>U</u>egf – <u>B</u>mp1; EGF, Epidermal Growth Factor; CCP, Complement Control Protein; SP, Serine Protease.

Identification of ErpB and ErpQ Binding Region on C1s

To determine the mechanism of inhibition I first sought to isolate the domains needed for full affinity interaction with ErpB and ErpQ. This was accomplished using an array of C1s domain truncations cumulatively making up physiologically available portions of the protein in the C1 complex. C1s contains 6 domains each contributing to the function and orientation of the molecule inside the C1 Complex (**Fig 14**). SPR analysis of 4 domain truncations with 2 different

38

serine protease activation states was used with immobilized $ErpQ_{19-343}$, $ErpQ_{168-343}$, and $ErpB_{138-378}$ (**Fig 15**). Domain truncations omitting the serine protease (SP) domain were incapable of high affinity interaction implicating its importance for binding. Furthermore, activation state was again shown to be a determinant for binding affinity as enzymes C1s CCP2-SP and C1s CCP1-CCP2-SP both bound to ErpB and ErpQ better than their proenzyme counterparts (**Fig 15**).Interestingly, there also seemed to be a conformational change in the C1s CCP1-CCP2-SP proenzyme form that made it significantly impaired to recognition compared to the C1s CCP2-SP proenzyme form that was consistent amongst all constructs (**Fig 15**). Although the domain truncation analysis identifies the SP domain as the major determinant for high affinity interaction it is only with the addition of the CCP1 domain that a WT-like conformational difference is seen. This difference must be in part be important to the binding of ErpB/Q to C1s and therefore should be included in subsequent analysis. However, even with the addition of the CCP1 domain and no detectable interaction with the other N-terminal domains, the affinities of C1s CCP2-SP and C1s CCP1-CCP2-SP enzymes do not fully replicate the binding affinities shown by C1s enzyme. This could be explained by low affinity interactions with N-terminal domains only in the presence of the SP domain thus proposing a two-step mechanism of binding, or possibly artificial C1s CCP1-CCP2-SP – C1s CCP1-CCP2-SP interactions sterically occluding CCP1 interactions in the proenzyme form that are alleviated in the enzyme form.

ErpQ$_{19-343}$

Legend:
- C1s Enzyme
- C1s CUB2-CCP1
- C1s CUB2-CCP1-CCP2
- C1s CCP2-SP Proenzyme
- C1s CCP2-SP Enzyme
- C1s CCP1-CCP2-SP Proenzyme
- C1s CCP1-CCP2-SP Enzyme

ErpQ$_{168-343}$

Legend:
- C1s Enzyme
- C1s CUB2-CCP1
- C1s CUB2-CCP1-CCP2
- C1s CCP2-SP Proenzyme
- C1s CCP2-SP Enzyme
- C1s CCP1-CCP2-SP Proenzyme
- C1s CCP1-CCP2-SP Enzyme

ErpB$_{138-378}$

Legend:
- C1s Enzyme
- C1s CUB2-CCP1
- C1s CUB2-CCP1-CCP2
- C1s CCP2-SP Proenzyme
- C1s CCP2-SP Enzyme
- C1s CCP1-CCP2-SP Proenzyme
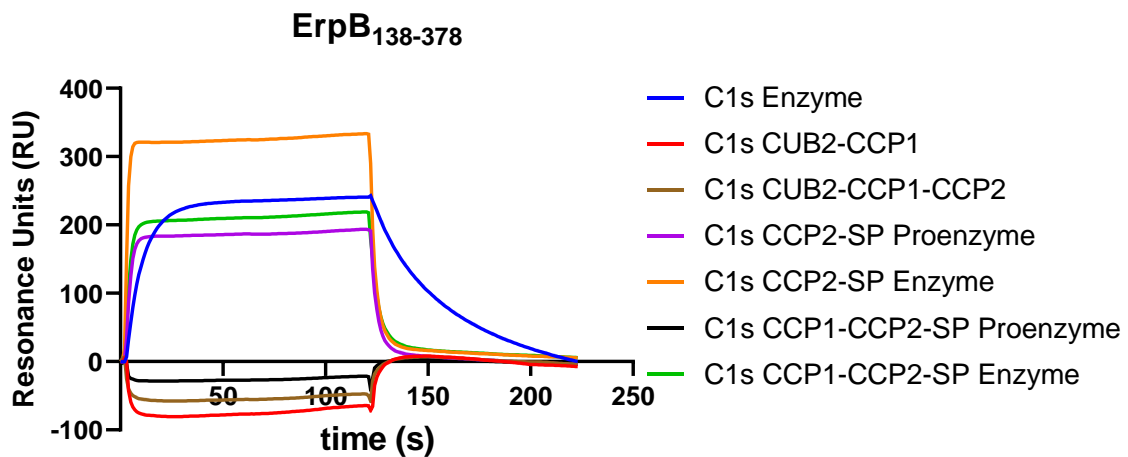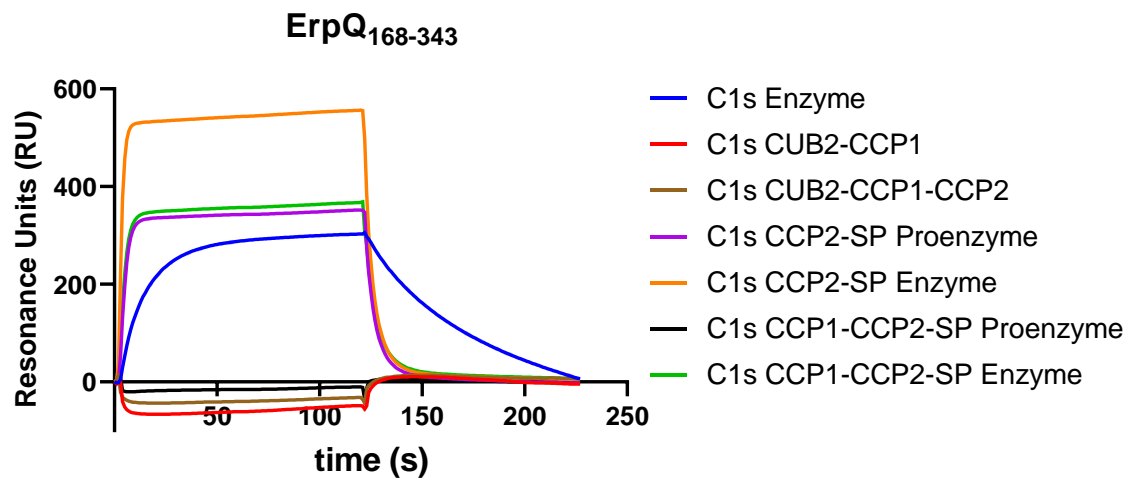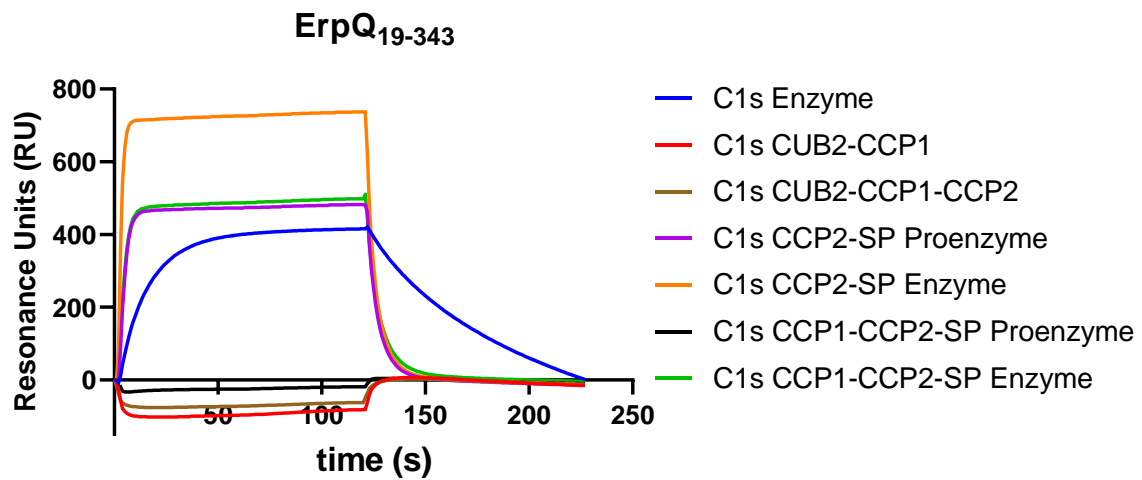- C1s CCP1-CCP2-SP Enzyme

40

Figure 15. ErpB and ErpQ bind the SP domain of C1s enzyme. Determination of C1s binding site with 6 domain truncations of C1s. SPR ranking study with 200 nM of each domain truncation injected over immobilized $ErpQ_{19-343}$, $ErpQ_{168-343}$, and $ErpB_{138-378}$. Analytes were injected for 120 sec association time and disassociated for 120 sec in HBS-T Ca^{2+}. Raw response curves were molecular weight corrected to C1s enzyme (86 kDa). SPR analysis is a representative curve set of triplicate experimentation.

ErpQ Does Not Interact with the Active Site of C1r or C1s

Given the affinity driven nature of the SP domain of C1s we then sought to understand the molecular mechanism of inhibition that ErpB and ErpQ are employing. As the SP domain contains the catalytic active site of the enzyme, we hypothesized that ErpB and ErpQ could be occluding the active site directly (**Appendix B**). To determine if this was the case, I employed the use of a colorimetric assay using small peptides that are specifically cleaved by C1r or C1s enzymes, respectfully. These peptides interact with the active site via $S_2-S_1-S'_1$ subsites of C1r and C1s, respectively[75]. Steric occlusion of these pockets by ErpB and ErpQ would interfere with proper recognition and orientation of the peptide over the catalytic site causing inhibition. Using $ErpQ_{19-343}$ as a surrogate for the inhibitory mechanism, I first tested the peptides with C1r CCP2-SP and the peptide Z-Gly-Arg-Thiobenzyl. Corroborating the previous C1s proenzyme activation assays (**Fig 11**) ErpQ was unable to inhibit C1r CCP2-SP cleavage of the peptide at 2.2 µM (22-fold higher than its K_D) (**Fig 16A**). BBK32-C, a C1r-specific active site inhibitor, and nafamostat mesylate (Futhan), an active site inhibitor of a range of proteases, were able to inhibit cleavage of the peptide. Subsequent analysis of C1s enzyme mediated cleavage of peptide Z-L-Lys-Thiobenzyl revealed that ErpQ was also unable to inhibit cleavage of the small peptide (**Fig**

41

16B). Together, these results implicate a novel mechanism of complement inhibition that works

outside of the active site.
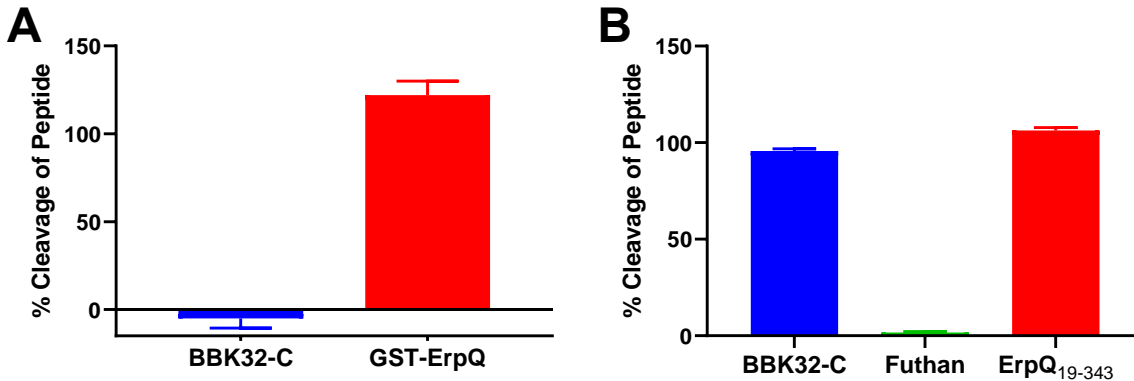
Figure 16. ErpQ is not able to block the cleavage of a small active site peptide in C1r or

C1s. A) To determine if ErpQ was capable of inhibiting the cleavage of a small peptide by the

active site of C1r a colorimetric enzyme assay was employed. 2.2 uM GST-ErpQ was added to

1.5 nM C1r CCP2-SP with 300 µM Z-Gly-Arg thiobenzyl ester and 100 µM DTNB at 25° C for

1 hr in HBS Ca^{2+}. Endpoint absorbance was read at 405 nm and BBK32-C was used as a control

for C1r inhibition at the same concentration. **B)** To determine if ErpQ was capable of inhibiting

the cleavage of a small peptide by the active site of C1s a similar colorimetric enzyme assay was

employed. 25 uM ErpQ$_{19-343}$ was added to 5 nM C1s enzyme with 300 µM Z-L-Lys thiobenzyl

ester and 100 µM DTNB at 25° C for 1 hr in HBS Ca^{2+}. Endpoint absorbance was read at 405

nm and BBK32-C was used as a negative control for C1s inhibition and futhan was used as a

positive control for C1s inhibition at the same concentrations.

ErpB and ErpQ Bind to a Known Exosite on C1s

To determine whether known exosites were involved with ErpB and ErpQ recognition of

C1s I prepared three C1s CCP1-CCP2-SP site-directed mutant (SDM) domain truncations. The

CCP1-CCP2-SP truncation was chosen as this construct had an affinity deficit in the proenzyme

form that was alleviated in the active form. Upon activation C1s has several conformational

changes in surface loops and CCP domains that enable the recognition of C4 (**Fig 16A**). These

regions of specificity outside of the active site are known as exosites. C1s is known to have at

least two exosites: i) an anion binding exosite (ABE) K575-R576-R581-K583, which is formed

for D loop facilitated recognition of an electrostatically negative region containing sulfotyrosine

residues on C4, and ii) a region between CCP1 and CCP2, hereafter "Hinge" (E326-D358),

which recognizes a region in the C345C domain of C4 (**Fig 17A**)[11,73].

Using this truncation allowed me to mutate each of the known C4-exosites in C1s, as well

as in tandem for a complete C1s C4-exosite deficient mutant. SPR analysis was then employed to

determine steady state affinities towards the mutated exosites compared to C1s CCP1-CCP2-SP

wild type (WT) (**Fig 17B**). SPR analysis indicated that exosite mutants containing the ABE

mutation were severely attenuated in binding of ErpB and ErpQ. This indicates that the ABE

residues K575-R576-R581-K583 collectively or individually contribute to high affinity

interactions with ErpB and ErpQ. Alternatively, the Hinge mutation was found to have only a

modest ~2-fold difference in affinity compared to WT in all Erp constructs (**Table 3**). These data

support that the C1s ABE is an important target for ErpB/Q mediated substrate inhibition. Being

that this exosite is important for recognition of C4 these data also support a plausible mechanism

A C1s Proenzyme | C1s Enzyme | ABE | Hinge

B
C1s Mutant Variants over ErpQ$_{19-343}$
C1s Mutant Variants over ErpQ$_{181-343}$
C1s Mutant Variants over ErpB$_{182-378}$

C
WT over ErpQ$_{19-343}$ | Hinge Mutant over ErpQ$_{19-343}$ | ABE Mutant over ErpQ$_{19-343}$ | ABE/Hinge Mutant over ErpQ$_{19-343}$
WT over ErpQ$_{181-343}$ | Hinge Mutant over ErpQ$_{181-343}$ | ABE Mutant over ErpQ$_{181-343}$ | ABE/Hinge Mutant over ErpQ$_{181-343}$
WT over ErpB$_{182-378}$ | Hinge Mutant over ErpB$_{182-378}$ | ABE Mutant over ErpB$_{182-378}$ | ABE/Hinge over ErpB$_{182-378}$
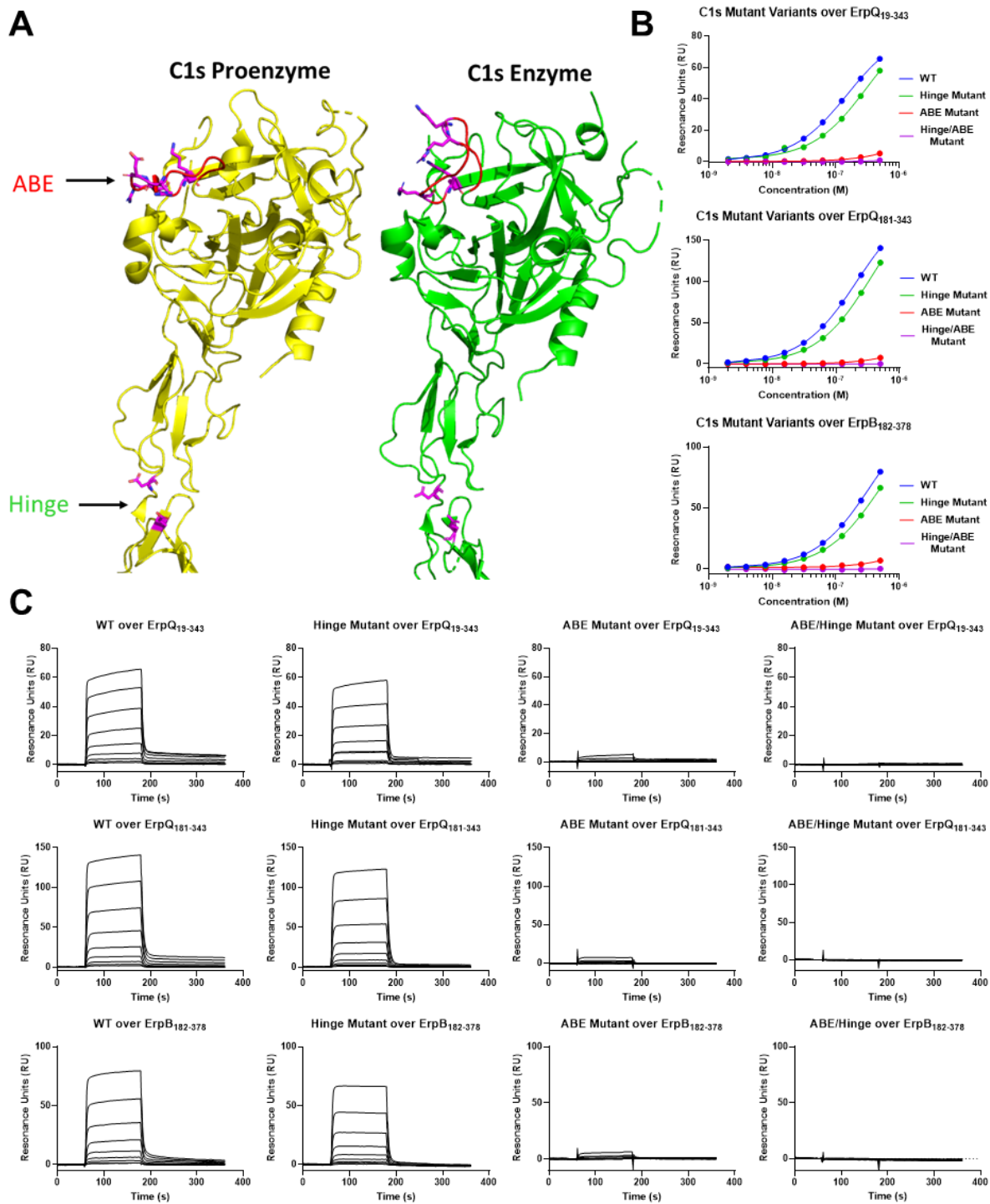
Figure 17. ErpB and ErpQ recognize an activation dependent anion binding exosite. A)
Cartoon structures of C1s in proenzyme and active states. C1s proenzyme (PDB:4J1Y, yellow) and C1s enzyme (PDB:5UBM, green) exhibit conformational changes upon activation. D loop conformational change is notated in red. Residues in purple represent amino acids that were mutated to alanine in the ABE (K575A-R576A-R581A-K583A), Hinge (E326A-D358A), or ABE/Hinge mutants (K575A-R576A-R581A-K583A, E326A-D358A). **B)** Steady state fits of corresponding analytes (**C**) injected over immobilized ErpQ$_{19-343}$, ErpQ$_{181-343}$, and ErpB$_{182-378}$. Fits were calculated with a 1:1 Langmuir model and shown on a logarithmic scale. **C)** Multi cycle SPR sensorgrams of C1s CCP1-CCP2-SP mutant variants binding to surface immobilized ErpB and ErpQ. Dose response curves were obtained with a twofold dilution (200-0.8 nM) in HBS-T Ca^{2+}. Sensorgrams and fits are a set representative of experiments performed in triplicate.

for enzyme inhibition outside of the active site through steric occlusion of an important exosite.

ErpQ and BBK32 Bind C1r Using a Non-Overlapping Binding Site

Although ErpB and ErpQ do not seem to inhibit C1r-mediated cleavage of C1s proenzyme they still form high affinity interactions that are conformationally sensitive. Due to the high similarity (57.6%) between the SP domains of C1r and C1s we hypothesized that the binding sites on C1r and C1s may be similar. Using an amplified luminescence proximity homogenous assay (ALPHA, **Appendix C**), I determined an appropriate amount of GST-ErpQ on donor beads to His-C1r CCP2-SP on acceptor beads for the Cheng-Prusoff equation to be applied where IC$_{50}$ approximates the K_D[71]. Using this system, I found that complement components dose-dependently competed for GST-ErpQ binding of His tagged C1r CCP2-SP, hereafter His-C1r CCP2-SP (**Fig 18A**). Within reasonable agreement of values obtained by SPR, His-C1r CCP2-SP competed with untagged C1 complex ($K_{D,ALPHA}$ = 1.7 nM, $K_{D,SPR}$ = 5.6 nM),

C1s enzyme ($K_{D,ALPHA}$ = 29 nM, $K_{D,SPR}$ = 3.9 nM), and C1r enzyme ($K_{D,ALPHA}$ = 120 nM, $K_{D,SPR}$ = 100 nM) for GST-ErpQ binding (**Fig 18A, Table 3**). Furthermore, C1q was also shown to not compete for GST-ErpQ binding in the presence of His-C1r CCP2-SP (K_D = n.d.) (**Fig 18A**). I then hypothesized that BBK32-C and ErpQ may bind C1 complex at the same time, so I designed an indirect ALPHA experiment to determine if both BBK32-C, which only interacts with C1r, and
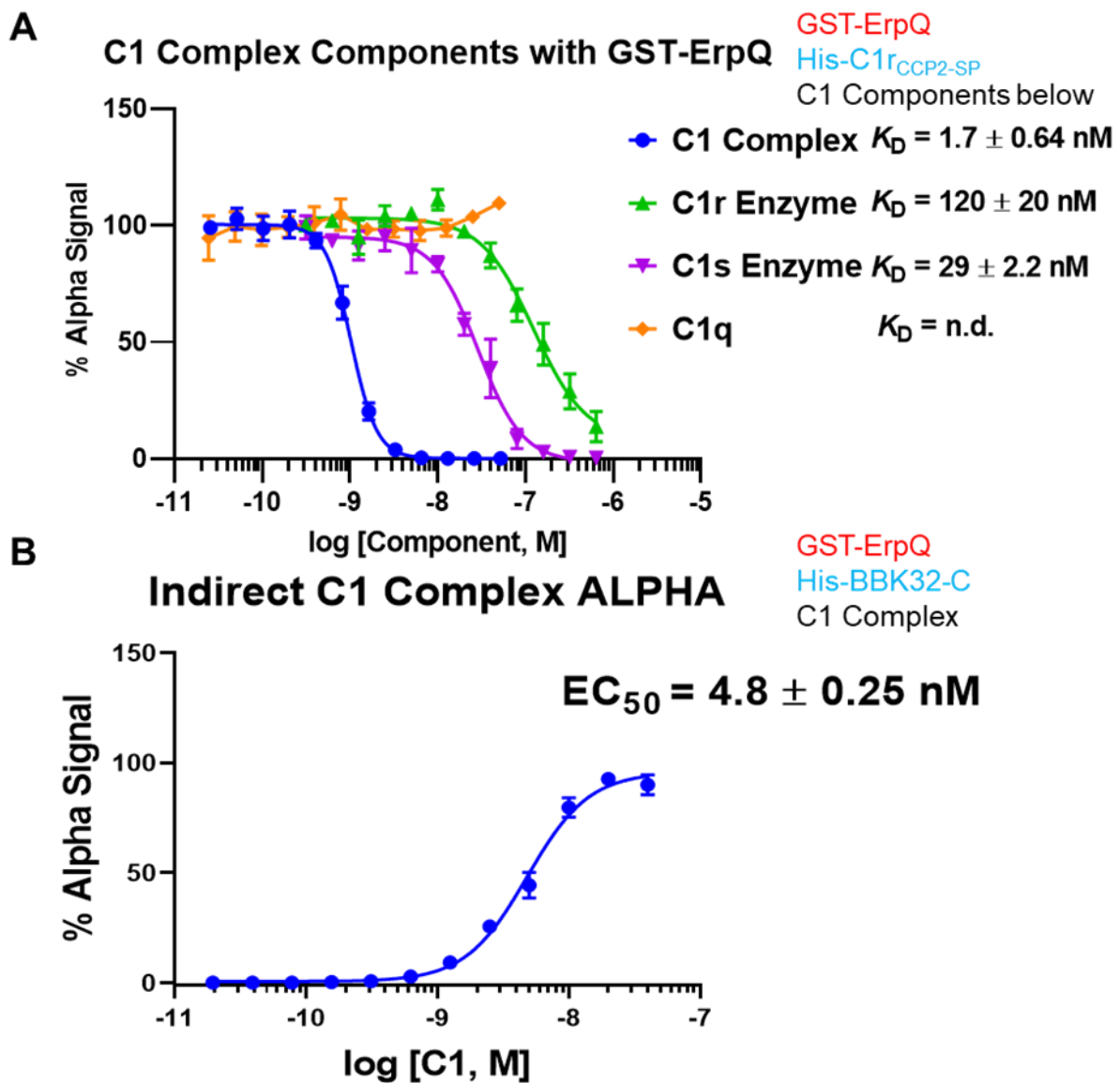
Figure 18. ErpQ competes with complement components but not BBK32-C for C1r-CCP2 SP binding. A) Direct ALPHA competition experiment with GST-ErpQ on donor beads (red) and His-C1r CCP2-SP on acceptor beads (cyan) shows competitive binding with titrated with C1 complex components. Twofold dilution of complement components at various concentrations was performed in HBS-T Ca^{2+}. C1 protease components, but not C1q were able to compete for ErpQ binding. **B)** Indirect ALPHA experiment with GST-ErpQ on donor beads (red) and His-BBK32-C on acceptor beads (cyan) shows simultaneous binding with titrated C1 complex. Twofold concentrations (40 – 0.02 nM) C1 complex was added to the reaction in HBS-T Ca^{2+}. ALPHA signal was normalized to positive and negative reactions with all experimentation performed in triplicate.

ErpQ, which can interact with either C1r or C1s, could bind C1 complex simultaneously. The formation of ALPHA signal indicates the binding of both His tagged BBK32-C, hereafter His-BBK32-C, and GST-ErpQ to the untagged ligand, C1 complex. GST-ErpQ and His-BBK32-C were able to generate signal at a half maximal effective concentration (EC_{50}) of 4.8 nM confirming that both BBK32-C and ErpQ can bind to C1 complex simultaneously (**Fig 18B**).

This was not necessarily surprising considering the ability for ErpQ to interact with the neighboring protease C1s. However, ErpQ is also able to bind C1r, therefore there was a possibility that ErpQ could be interacting on the C1r subcomponent with BBK32-C. To test whether GST-ErpQ has overlapping binding sites on His-C1r CCP2-SP with BBK32-C I employed the use of a direct ALPHA. Interestingly, there was no observable competition between BBK32-C and GST-ErpQ binding of His-C1r CCP2-SP at concentrations well above the K_D's for each inhibitor (**Fig 19A**). To validate this result, I developed an indirect ALPHA to have untagged full length C1r enzyme to generate signal with GST-ErpQ and His-BBK32-C.

Corroborating results from the direct ALPHA, addition of C1r enzyme in the presence of GST-ErpQ and His-BBK32-C elicited a robust response (EC_{50} = 27 nM) (**Fig 18B**). Collectively this
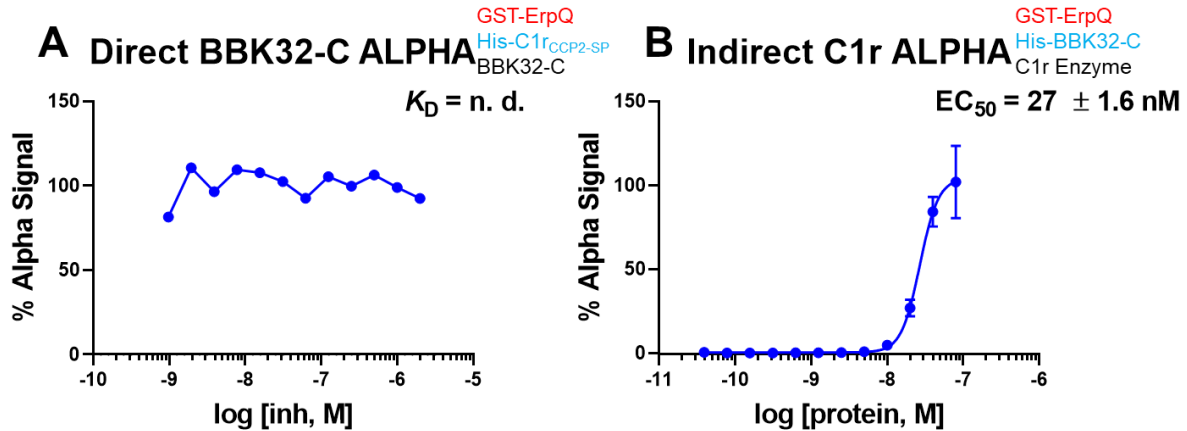
Figure 19. ErpQ has a non-overlapping binding site with BBK32-C on C1r. A) Direct ALPHA with GST-ErpQ on donor beads (red) and His-C1r CCP2-SP on acceptor beads (cyan) shows no competition by BBK32-C addition. Twofold concentrations of BBK32-C (2000 – 1 nM) were added to compete with GST-ErpQ and His-C1r CCP2-SP interaction in HBS-T Ca^{2+}. **B)** Indirect ALPHA with GST-ErpQ on donor beads (red) and His-C1r CCP2-SP on acceptor beads (cyan) with signal generated by the addition of common ligand C1r enzyme. Twofold dilution of C1r enzyme (80 – 3.9 nM) was added to GST-ErpQ and His-C1r CCP2-SP reaction in HBS-T Ca^{2+}. Indirect ALPHA was performed in triplicate.

indicated that it was possible for BBK32-C and ErpQ to bind C1r simultaneously in the C1 complex. Upon inspection of the recently "pre-printed" small x-ray scattering structure of BBK32-C in complex with C1r CCP2-SP, the D loop contains only three contact residues with none of them conserved amongst both C1r and C1s (**Fig 20**)[52]. However, C1r does contain two basic amino acids corresponding to amino acids shown to be important for ErpB and ErpQ

binding: K602-R608, which correspond to similarly basic R576-K583 on C1s. This indicates that

the conserved necessary high affinity amino acids in the ABE of C1s are available in the C1r D

```
C1r_SP_Domain_464-705_    IIGGQKAKMGNFPWQVFTNIHGRGGGALLGDRWILTAAHTLYPKEHEAQSNASLDVHLGH
C1s_SP_Domain_438-688_    IIGGSDADIKNFPWQVFFDNP-WAGGALINEYWVLTAAHVVEGNRE-------PTMYVGS
                          ****..*.: ******* :    .****:.: *:*****.:  :..        :::*

C1r_SP_Domain_464-705_    TNVE--ELMKLGNHPIRRVSVHPDYR----QDESYNREGDIALLELENSVTLGPNLLPIC
C1s_SP_Domain_438-688_    TSVQTSRLAKSKMLTPEHVFIHPGWKLLEVPEGRTNFDNDIALVRLKDPVKMGPTVSPIC
                          *.*:  .* *       .:* :**.::    :   **:.****:.*:: *.:**.: ***
                                                          D Loop
C1r_SP_Domain_464-705_    LPDNDTFYDL--GLMGYVSGFGVMEEK-IAHDLRFVRLPVANPQACENWLRGK----NRM
C1s_SP_Domain_438-688_    LPGTSSDYNLMDGDLGLISGWGRTEKRDRAVRLKAARLPVAPLRKCKEVKVEKPTADAEA
                          **...: *:*   * :* :**:*  *::  *  *: .*****  : *::    *    .

C1r_SP_Domain_464-705_    DVFSQNMFCAGHPSLKQDACQGDSGGVFAVRDPNT-DRWVATGIVSWGIGCSRGYGFYTK
C1s_SP_Domain_438-688_    YVFTPNMICAGGE-KGMDSCKGDSGGAFAVQDPNDKTKFYAAGLVSWGPQCG-TYGLYTR
                           **: **:***    *:*:**.***:*** :: *:*:**** *. **:**:

C1r_SP_Domain_464-705_    VLNYVDWIKKEMEEED-----
C1s_SP_Domain_438-688_    VKNYVDWIMKTMQENSTPRED
                          * ****** * *:*:.
```

Figure 20. BBK32-C does not interact with residues similar to the ABE in C1s. Pairwise alignment of SP domains of C1r and C1s. Catalytic triad colored as blue asterisks, contact residues with BBK32-C are highlighted in red, and C1s ABE mutant residues highlighted in yellow. Figure was adapted from Garrigues et al. 2021[52].

Loop. However, using the C1r CCP2-SP also includes a conserved construct D375 (D358, C1s

numbering), which is one of the two amino acids in the C1s Hinge mutant. Altogether, these

results indicate that none of the suspected amino acids that ErpQ interacts with are bound by

BBK32-C.

49

CHAPTER 5: DISSCUSSION

Borreliella spirochetes cause nearly 476, 000 new cases of Lyme Disease per year in the US with estimates of PTLDS capping nearly 2 million in some analyses[42,76]. Cumulatively these staggering statistics make Lyme Disease the number one vector-borne illness in the US. Aspects of its pathogenesis, epidemiology, and vaccination are being pursued to reduce adverse financial and health outcomes caused by Lyme Disease[77,78]. The ability of Borreliella spirochetes to disseminate through the vasculature has attracted much attention to their ability to inhibit and evade innate immune responses such as the complement system[43,44]. These evasion mechanisms provide key insights into the overall pathogenesis of Borreliella and offer perspective on potential vaccination targets.

The alternative and classical pathways have each been implicated in the successful complement-mediated destruction of Borreliella. To protect against the host innate immune response, Lyme disease causing spirochetes have evolved highly redundant and mechanistically distinct proteins for the defense and evasion of the complement system (**Fig 2**)[44]. A primary evasion mechanism is decorating their surface with negative regulators of complement like FH, FI, or C4BP[1]. Borreliella achieve this through CRASPs ErpA, ErpP, CspA, CspZ and p43, which bind to negative complement regulators in such a way that they are able to inhibit further deposition of complement products[45,79]. In addition to this repertoire, expression of direct inhibitors BBK32 and OspC target C1r and C4b, respectively[51,80]. BBK32 inhibits C1r holding it in a zymogen state, as well as acts as a potent active site inhibitor[51,52]. OspC binds to C4b and competes with binding of C2, thereby blocking the formation of the CP/LP C3 convertase negative influencing either CP or LP activation[80]. If complement activation has overwhelmed these upstream defenses, Borreliella also expresses four proteins that inhibit the formation of

MAC CspA, BGA66, BGA71, and a CD59-like protein[43]. CspA, which also binds FH, can inhibit formation of MAC directly through interactions with C7 and interrupting the polymerization of C9[48]. *B. bavariensis* expresses BGA66 and BGA71, which like CspA also bind C7 and C9, but also interact with C8 and inhibit the formation of MAC[47]. Finally, a CD59-like protein has been shown to perform CD59-like functions of MAC inhibition, but has not yet been fully described[49].

Studies completed in complement deficient mice have shown classical pathway and alternative pathway significance upstream of C5[56–58,60]. However, naïve serum in the presence of *B. burgdorferi* has long been known to activate CP and AP *in vitro* leading to complement activation of the pathways but resistance to killing[81]. Upon addition of specific antibody spirochetes were immediately killed via the CP[81]. This paradox could be in part explained by low affinity interactions with non-canonical ligands that could activate C1 on the surface of *Borreliella* but does not explain why host-mediated Lyme clearance is not achieved. Work contributing to the interactome between complement and these spirochetes can better describe the implications certain vaccines may have on *Borreliella.*

In addition to these studies, complement is further implicated in host range specificities across *Borreliella*[82]. Cumulatively this repertoire indicates a severe requirement for *Borreliella* to produce and keep these proteins as a basis for survival in plasma and contributes to the overall pathogenesis of *Borreliella*[43]. However, only recently have we had tools to investigate the surface lipoproteome for further interactions with important immune surveillance proteins[46,67]. Our collaborators in Dr. John Leong's lab described the discovery of two novel proteins that interacted with C1 complex through a gain-of-function library screen[67]. The results of the study presented herein describes the role of ErpB and ErpQ in *Borreliella* protection from CP-

mediated cell killing through the inhibition of C1s. A multipronged approach was used to determine the function of ErpB and ErpQ to interact with C1 complex. ErpB and ErpQ were found to bind with high affinity to both C1 complex proteases C1r and C1s and further study indicated that the SP domains of C1r and C1s were important for these interactions. Proteolytic cleavage assays showed that ErpB and ErpQ inhibit C1s-mediated cleavage of natural substrates, but not C1r. Interestingly, although both inhibitors bound the SP domains neither ErpB nor ErpQ was able to inhibit the active site when small peptide was introduced. C1s C4-exosite mutants then revealed that one of the main affinity drivers for ErpB and ErpQ interactions lies in a conformationally sensitive C4-exosite only presented in the enzyme conformation of C1s. Analysis of SPR data confirmed that ErpB and ErpQ were sensitive to activation states of both C1r and C1s. Finally the inhibitory domain of ErpB and ErpQ was found to reside in the C-terminus of both proteins similarly to BBK32[50]. In an effort to further describe the binding site of ErpQ, we found that ErpQ and BBK32-C were able to bind to C1r CCP2-SP simultaneously[52]. Further structural studies will need to be conducted to fully describe the C1s mechanism of inhibition as well as *in vivo* knock-out approaches to determine the roles of ErpB and ErpQ in borrelial pathogenesis.

In addition to its ability to inhibit one of the serine protease components of the C1 complex, C1r, BBK32 has also been described to have multiple nonoverlapping sites enabling it to bind both fibronectin and glycosaminoglycans (GAGs)[51,83,84]. This multi-functional characteristic is described elsewhere in *Borrelia*. For example CspA, from *Borreliella*, and BhCRASP-1, from Relapsing fever spirochete *B. hermsii*, have both been shown to bind FH and plasminogen[48,85,86]. Though the nature of these interactions has been implicated to both impact the degradation of C3b in some species and not others currently it is thought that the use of

plasmin(ogen) is for cleaving extracellular matrix (ECM) proteins to aid in borrelial mobility[85].Other important human pathogens such as *Staphylococcus aureus* have combined multifunctional complement inhibitors, where the secretion of an extracellular fibrinogen binding protein (Efb) allows *S. aureus* to bind fibrinogen and C3b simultaneously[87]. In this case, fibrinogen is used to create a fibrinogen shield to aid in evasion from phagocytosis supporting a key role in control of both adaptive and innate immune responses in tandem to ensure survival[87,88]. This model of dual functionality may also extend to ErpB/Q, which may have a separate function in the N-terminal 160 amino acids that were found to not inhibit C4b deposition. Future studies should be directed at functionality in this region of the protein including binding to extracellular proteins that may aid in adherence to the extracellular environment, adhesins.

To date, there has only been one non-host derived CP-specific inhibitor, BBK32[89]. However, recently Pang et al. characterized a CP/LP inhibitor, gigastasin, made by the hematophagous giant amazon leech[51,70]. Like BBK32, gigastasin is an active site inhibitor, but it is capable of inhibition of C1s, MASP-2, and MASP-1 through the interaction of the ABE[70]. Interestingly, gigastasin is a poor inhibitor of C1r, making the mechanism of action specific to the proteases capable of cleaving C2. Taken together with the results presented in this study we present a molecule that specifically inhibits the CP, but similarly binds to the ABE on C1s. This example of convergent evolution to inhibit C1s activation of downstream components demonstrates the importance of the function of the ABE in substrate recognition. Thus, underpinning the significance of the study of inhibitors as tools to investigate protease function.

Complement dysregulation has long been implicated in a variety of diseases including systemic lupus erythematosus (SLE), paroxysmal nocturnal hemoglobinuria (PNH), hereditary

angioedema (HAE), heparin induced thrombocytopenia (HIT), cold agglutinin disease (CAD), Alzheimer disease (AD), atypical hemolytic uremic syndrome (aHUS) and many other diseases[3,11]. Therefore different activation steps have been the target of complement-related therapeutics[68,90]. Currently there are only two approved complement-targeted therapeutics, C1-INH and eculizumab[91]. C1-INH approved for therapeutic use is isolated in one of two ways i) isolated from whole blood product under the trade name Cinryze® (Takeda Pharmaceutical) or ii) produced recombinantly in rabbits under the trade name Ruconest® (Pharming Healthcare)[92,93]. Both preparations are approved for the treatment of acute HAE. Eculizumab, sold under the trade name Soliris® (Alexion Pharmaceuticals), is a monoclonal antibody raised against C5 preventing its cleavage and downstream effector functions that has been approved for clinical use in PNH, aHUS, and general myasthenia gravis (gMG)[94,95]. In addition to these a more recent monoclonal antibody raised against protease C1s, Sutimlimab (BIV009, Sanofi), is in ongoing phase III clinical trials for CAD[96]. By studying host interaction with borrelial inhibitors, we can find new ways to target certain pathways of complement making more efficient and potent therapeutics.

Collectively the data presented in this study support the high level of redundancy that *Borreliella* has toward complement inhibition and furthers our understanding of the Lyme-immune interactome. To our knowledge, ErpB and ErpQ represent the first microbial C1s specific inhibitors, which also have a novel mechanism of classical pathway-specific complement inhibition. Further study of these proteins, as well as other naturally occurring complement inhibitors provides us with insight and targets for the development of potent and specific therapeutics for complement related diseases.

References

1. Merle NS, Church SE, Fremeaux-Bacchi V, Roumenina LT. Complement system part I - molecular mechanisms of activation and regulation. *Front Immunol*. 2015;6(JUN):262. doi:10.3389/fimmu.2015.00262

2. Bohlson SS, Garred P, Kemper C, Tenner AJ. Complement nomenclature-deconvoluted. *Front Immunol*. 2019;10(JUN):1-6. doi:10.3389/fimmu.2019.01308

3. Merle NS, Noe R, Halbwachs-Mecarelli L, Fremeaux-Bacchi V, Roumenina LT. Complement system part II: Role in immunity. *Front Immunol*. 2015;6(MAY):1-26. doi:10.3389/fimmu.2015.00257

4. Ziccardi RJ. The first component of human complement (C1): Activation and control. *Springer Semin Immunopathol*. 1983;6(2-3):213-230. doi:10.1007/BF00205874

5. Ugurlar D, Howes SC, Kreuk B De, et al. Structures of C1-IgG1 provide insights into howdanger pattern recognition activates complement. *ACS Nano*. 2018;797(February):794-797.

6. Sharp TH, Boyle AL, Diebolder CA, Kros A, Koster AJ, Gros P. Insights into IgM-mediated complement activation based on in situ structures of IgM-C1-C4b. *Proc Natl Acad Sci U S A*. 2019;116(24):11900-11905. doi:10.1073/pnas.1901841116

7. Krishnan V, Xu Y, Macon K, Volanakis JE, Narayana SVL. The structure of C2b, a fragment of complement component C2 produced during C3 convertase formation. *Acta Crystallogr Sect D Biol Crystallogr*. 2009;65(3):266-274. doi:10.1107/S0907444909000389

8. Zwarthoff SA, Berends ETM, Mol S, et al. Functional characterization of alternative and classical pathway C3/C5 convertase activity and inhibition using purified models. *Front Immunol*. 2018;9(JUL):1-13. doi:10.3389/fimmu.2018.01691

9. Garred P, Genster N, Pilely K, et al. A journey through the lectin pathway of complement—MBL and beyond. *Immunol Rev*. 2016;274(1):74-97. doi:10.1111/imr.12468

10. Héja D, Kocsis A, Dobó J, et al. Revised mechanism of complement lectin-pathway activation revealing the role of serine protease MASP-1 as the exclusive activator of MASP-2. *Proc Natl Acad Sci*. 2012;109(26):10498-10503. doi:10.1073/PNAS.1202588109

11. Kidmose RT, Laursen NS, Dobó J, et al. Structural basis for activation of the complement system by component C4 cleavage. *Proc Natl Acad Sci U S A*. 2012;109(38):15425-15430. doi:10.1073/pnas.1208031109

12. Forneris F, Ricklin D, Wu J, et al. Structures of C3b in complex with factors B and D give insight into complement convertase formation. *Science (80-)*. 2010;330(6012):1816-1820. doi:10.1126/science.1195821

13. Serna M, Giles JL, Morgan BP, Bubeck D. Structural basis of complement membrane

attack complex formation. *Nat Commun*. 2016;7:1-7. doi:10.1038/ncomms10587

14.   Klos A, Tenner AJ, Johswich KO, Ager RR, Reis ES, Köhl J. The role of the anaphylatoxins in health and disease. *Mol Immunol*. 2009;46(14):2753-2766. doi:10.1016/j.molimm.2009.04.027

15.   Hourcade D, Post TW, Holers VM, Lublin DM, Atkinson JP. Polymorphisms of the regulators of complement activation gene cluster. *Complement Inflamm*. 1990;7(4-6):302-314. doi:10.1159/000463165

16.   Beinrohr L, Murray-Rust TA, Dyksterhuis L, et al. Serpins and the complement system. *Methods Enzymol*. 2011;499:55-75. doi:10.1016/B978-0-12-386471-0.00004-3

17.   Ambrus G, Gál P, Kojima M, et al. Natural Substrates and Inhibitors of Mannan-Binding Lectin-Associated Serine Protease-1 and -2: A Study on Recombinant Catalytic Fragments. *J Immunol*. 2003;170(3):1374-1382. doi:10.4049/jimmunol.170.3.1374

18.   Silverman GA, Whisstock JC, Bottomley SP, et al. Serpins flex their muscle: I. Putting the clamps on proteolysis in diverse biological systems. *J Biol Chem*. 2010;285(32):24299-24305. doi:10.1074/jbc.R110.112771

19.   Whisstock JC, Silverman GA, Bird PI, et al. Serpins flex their muscle: II. Structural insights into target peptidase recognition, polymerization, and transport functions. *J Biol Chem*. 2010;285(32):24307-24312. doi:10.1074/jbc.R110.141408

20.   Ziccardi RJ. A new role for C-1-inhibitor in homeostasis : control of activation of the first component of human complement. *J Immunol*. 1982;128(6):2505-2508.

21.   Yin C, Ackermann S, Ma Z, et al. ApoE attenuates unresolvable inflammation by complex formation with activated C1q. *Nat Med*. 2019;25(3):496-506. doi:10.1038/s41591-018-0336-8

22.   Cong Q, Soteros BM, Wollet M, Kim JH, Sia GM. The endogenous neuronal complement inhibitor SRPX2 protects against complement-mediated synapse elimination during development. *Nat Neurosci*. 2020;23(September). doi:10.1038/s41593-020-0672-0

23.   Kerr FK, O'Brien G, Quinsey NS, et al. Elucidation of the substrate specificity of the C1s protease of the classical complement pathway. *J Biol Chem*. 2005;280(47):39510-39514. doi:10.1074/jbc.M506131200

24.   Villiers MB, Thielens NM, Colomb MG. Soluble C3 proconvertase and convertase of the classical pathway of human complement. Conditions of stabilization in vitro. *Biochem J*. 1985;226(2):429-436. doi:10.1042/bj2260429

25.   Kerr MA. *Complement Component C2: The Classical and Lectin Pathway C3/C5 Convertases*. Vol 3.; 2013. doi:10.1016/B978-0-12-382219-2.00634-7

26.   Feng S, Liang X, Kroll MH, Chung DW, Afshar-Kharghan V. Von willebrand factor is a cofactor in complement regulation. *Blood*. 2015;125(6):1034-1037. doi:10.1182/blood-2014-06-585430

27.   Lambris JD, Lao Z, Oglesby TJ, Atkinson JP, Hack CE, Becherer JD. Dissection of CR1,

factor H, membrane cofactor protein, and factor B binding and functional sites in the third complement component. *J Immunol*. 1996;156(12):4821-4832. http://www.ncbi.nlm.nih.gov/pubmed/8648130.

28.   Jenne DE, Tschopp J. Molecular structure and functional characterization of a human complement cytolysis inhibitor found in blood and seminal plasma: identity to sulfated glycoprotein 2, a constituent of rat testis fluid. *Proc Natl Acad Sci U S A*. 1989;86(18):7123-7127. doi:10.1073/pnas.86.18.7123

29.   Sheehan M, Morris CA, Pussell BA, Charlesworth JA. Complement inhibition by human vitronectin involves non-heparin binding domains. *Clin Exp Immunol*. 1995;101(1):136-141. doi:10.1111/j.1365-2249.1995.tb02289.x

30.   Huang Y, Fedarovich A, Tomlinson S, Davies C. Crystal structure of CD59: Implications for molecular recognition of the complement proteins C8 and C9 in the membrane-attack complex. *Acta Crystallogr Sect D Biol Crystallogr*. 2007;63(6):714-721. doi:10.1107/S0907444907015557

31.   Steere AC, Malawista SE, Snydman DR, et al. An epidemic of oligoarticular arthritis in children and adults in three connecticut communities. *Arthritis Rheum*. 1977;20(1):7-17. doi:10.1002/art.1780200102

32.   Burgdorfer W. Discovery of the Lyme disease spirochete and its relation to tick vectors. *Yale J Biol Med*. 1984;57(4):515-520.

33.   Burgdorfer W, Barbour A, Hayes S, Benach J, Grunwaldt E, Davis J. Lyme disease-a tick-borne spirochetosis? *Science (80-)*. 1982;216(4552):1317-1319. doi:10.1126/science.7043737

34.   Adeolu M, Gupta RS. A phylogenomic and molecular marker based proposal for the division of the genus Borrelia into two genera: The emended genus Borrelia containing only the members of the relapsing fever Borrelia, and the genus Borreliella gen. nov. containing the members o. *Antonie van Leeuwenhoek, Int J Gen Mol Microbiol*. 2014;105(6):1049-1072. doi:10.1007/s10482-014-0164-x

35.   Gupta RS. Distinction between Borrelia and Borreliella is more robustly supported by molecular and phenotypic characteristics than all other neighbouring prokaryotic genera: Response to Margos' et al. "The genus Borrelia reloaded" (PLoS ONE 13(12): E0208432). *PLoS One*. 2019;14(8):1-22. doi:10.1371/journal.pone.0221397

36.   Rudenko N, Golovchenko M, Grubhoffer L, Oliver JH. Updates on borrelia burgdorferi sensu lato complex with respect to public health. *Ticks Tick Borne Dis*. 2011;2(3):123-128. doi:10.1016/j.ttbdis.2011.04.002

37.   Charon NW, Cockburn A, Li C, et al. The unique paradigm of spirochete motility and chemotaxis. *Annu Rev Microbiol*. 2012;66(1912):349-370. doi:10.1146/annurev-micro-092611-150145

38.   Radolf JD, Caimano MJ, Stevenson B, Hu LT. Of ticks, mice and men: Understanding the dual-host lifestyle of Lyme disease spirochaetes. *Nat Rev Microbiol*. 2012;10(2):87-99. doi:10.1038/nrmicro2714

39. Bush LM, Vazquez-Pertejo MT. Tick borne illness—Lyme disease. *Disease-a-Month*. 2018;64(5):195-212. doi:10.1016/j.disamonth.2018.01.007

40. Rebman AW, Aucott JN. Post-treatment Lyme Disease as a Model for Persistent Symptoms in Lyme Disease. *Front Med*. 2020;7(February):1-16. doi:10.3389/fmed.2020.00057

41. Moore A, Nelson C, Molins C, Mead P, Schriefer M. Current guidelines, common clinical pitfalls, and future directions for laboratory diagnosis of lyme disease, United States. *Emerg Infect Dis*. 2016;22(7):1169-1177. doi:10.3201/eid2207.151694

42. Kugeler KJ, Schwartz AM, Delorey MJ, Mead PS, Hinckley AF. Estimating the frequency of lyme disease diagnoses, United States, 2010-2018. *Emerg Infect Dis*. 2021;27(2):616-619. doi:10.3201/eid2702.202731

43. Coburn J, Garcia B, Hu LT, et al. Lyme Disease Pathogenesis. *Lyme Dis Relapsing Fever Spirochetes Genomics, Mol Biol Host Interact Dis Pathog*. 2021;42:473-518. doi:10.21775/9781913652616.13

44. Skare JT, Garcia BL. Complement Evasion by Lyme Disease Spirochetes. *Trends Microbiol*. 2020:1-11. doi:10.1016/j.tim.2020.05.004

45. Kraiczy, Peter; Stevenson B. Complement regulator-acquiring surface proteins of Borrelia burgdorferi: Structure, function and regulation of gene expression. 2014;27(4):1-19. doi:10.1037/a0032811.Child

46. Dowdell AS, Murphy MD, Azodi C, et al. Comprehensive spatial analysis of the Borrelia burgdorferi lipoproteome reveals a compartmentalization bias toward the bacterial surface. *J Bacteriol*. 2017;199(6):1-20. doi:10.1128/JB.00658-16

47. Hammerschmidt C, Klevenhaus Y, Koenigs A, et al. BGA66 and BGA71 facilitate complement resistance of Borrelia bavariensis by inhibiting assembly of the membrane attack complex. *Mol Microbiol*. 2016;99(2):407-424. doi:10.1111/mmi.13239

48. Hallström T, Siegel C, Mörgelin M, Kraiczy P, Skerka C, Zipfel PF. CspA from Borrelia burgdorferi inhibits the terminal complement pathway. *MBio*. 2013;4(4):1-10. doi:10.1128/mBio.00481-13

49. Pausa M, Pellis V, Cinco M, et al. Serum-Resistant Strains of Borrelia burgdorferi Evade Complement-Mediated Killing by Expressing a CD59-Like Complement Inhibitory Molecule . *J Immunol*. 2003;170(6):3214-3222. doi:10.4049/jimmunol.170.6.3214

50. Xie J, Zhi H, Garrigues RJ, Keightley A, Garcia BL, Skare JT. Structural determination of the complement inhibitory domain of borrelia burgdorferi BBK32 provides insight into classical pathway complement evasion by lyme disease spirochetes. *PLoS Pathog*. 2019;15(3). doi:10.1371/journal.ppat.1007659

51. Garcia BL, Zhi H, Wager B, Höök M, Skare JT. Borrelia burgdorferi BBK32 Inhibits the Classical Pathway by Blocking Activation of the C1 Complement Complex. *PLoS Pathog*. 2016;12(1):1-28. doi:10.1371/journal.ppat.1005404

52. Garrigues RJ, Powell AD, Hammel M. A structural basis for inhibition of the complement

initiator protease C1r by Lyme disease spirochetes. *bioRxiv Microbiol*. 2021. http://biorxiv.org/cgi/content/short/2021.01.21.427683v1?rss=1&utm_source=researcher_app&utm_medium=referral&utm_campaign=RESR_MRKT_Researcher_inbound.

53. Pangburn MK, Schreiber RD, Müller-Eberhard HJ. Human complement C3b inactivator: isolation, characterization, and demonstration of an absolute requirement for the serum protein beta1H for cleavage of C3b and C4b in solution. *J Exp Med*. 1977;146(1):257-270. doi:10.1084/jem.146.1.257

54. Clark SJ, Schmidt CQ, White AM, Hakobyan S, Morgan BP, Bishop PN. Identification of Factor H–like Protein 1 as the Predominant Complement Regulator in Bruch's Membrane: Implications for Age-Related Macular Degeneration. *J Immunol*. 2014;193(10):4962-4970. doi:10.4049/jimmunol.1401613

55. Makou E, Herbert AP, Barlow PN. Functional anatomy of complement factor H. *Biochemistry*. 2013;52(23):3949-3962. doi:10.1021/bi4003452

56. Zhi H, Xie J, Skare JT. The classical complement pathway is required to control Borrelia burgdorferi levels during experimental infection. *Front Immunol*. 2018;9(MAY):1-12. doi:10.3389/fimmu.2018.00959

57. Lawrenz MB, Wooten RM, Zachary JF, et al. Effect of complement component C3 deficiency on experimental lyme borreliosis in mice. *Infect Immun*. 2003;71(8):4432-4440. doi:10.1128/IAI.71.8.4432-4440.2003

58. Woodman ME, Cooley AE, Miller JC, et al. Borrelia burgdorferi binding of host complement regulator factor H is not required for efficient mammalian infection. *Infect Immun*. 2007;75(6):3131-3139. doi:10.1128/IAI.01923-06

59. Brissette CA, Cooley AE, Burns LH, et al. Lyme borreliosis spirochete Erp proteins, their known host ligands, and potential roles in mammalian infection. *Int J Med Microbiol*. 2008;298(SUPPL. 1):257-267. doi:10.1016/j.ijmm.2007.09.004

60. Bockenstedt LK, Barthold S, Deponte K, Marcantonio N, Kantor FS. Borrelia burgdorferi infection and immunity in mice deficient in the fifth component of complement. *Infect Immun*. 1993;61(5):2104-2107. doi:10.1128/iai.61.5.2104-2107.1993

61. Jensen RA. Orthologs and paralogs - We need to get it right (multiple letters) [1]. *Genome Biol*. 2001;2(8):1-3. doi:10.1186/gb-2001-2-8-interactions1002

62. Casjens S, Palmer N, Van Vugt R, et al. A bacterial genome in flux: The twelve linear and nine circular extrachromosomal DNAs in an infectious isolate of the Lyme disease spirochete Borrelia burgdorferi. *Mol Microbiol*. 2000;35(3):490-516. doi:10.1046/j.1365-2958.2000.01698.x

63. Akins DR, Porcella SF, Popova TG, et al. Evidence for in vivo but not in vitro expression of a Borrelia burgdorferi outer surface protein F (OspF) homologue. *Mol Microbiol*. 1995;18(3):507-520. doi:10.1111/j.1365-2958.1995.mmi_18030507.x

64. Hefty PS, Jolliff SE, Caimano MJ, Wikel SK, Radolf JD, Akins DR. Regulation of OspE-related, OspF-related, and Elp lipoproteins of Borrelia burgdorferi strain 297 by mammalian host-specific signals. *Infect Immun*. 2001;69(6):3618-3627.

doi:10.1128/IAI.69.6.3618-3627.2001

65. Stevenson B, Bono JL, Schwan TG, Rosa P. Borrelia burgdorferi Erp proteins are immunogenic in mammals infected by tick bite, and their synthesis is inducible in cultured bacteria. *Infect Immun*. 1998;66(6):2648-2654. doi:10.1128/iai.66.6.2648-2654.1998

66. Akins DR, Caimano MJ, Yang X, Cerna F, Norgard M V., Radolf JD. Molecular and evolutionary analysis of Borrelia burgdorferi 297 circular plasmid-encoded lipoproteins with OspE- and OspF-like leader peptides. *Infect Immun*. 1999;67(3):1526-1532. doi:10.1128/iai.67.3.1526-1532.1999

67. Pereira MJ. The Borrelia burgdorferi lipoproteins ErpB and ErpQ promote spirochetal binding to the human complement C1 protein complex and inhibit initiation of the classical complement cascade. 2020;(February).

68. Rushing BR, Rohlik DL, Roy S, Skaff DA, Garcia BL. Targeting the Initiator Protease of the Classical Pathway of Complement Using Fragment-Based Drug Discovery. *Molecules*. 2020;25(17). doi:10.3390/molecules25174016

69. Kardos J, Gál P, Szilágyi L, et al. The Role of the Individual Domains in the Structure and Function of the Catalytic Region of a Modular Serine Protease, C1r. *J Immunol*. 2001;167(9):5202-5208. doi:10.4049/jimmunol.167.9.5202

70. Pang SS, Wijeyewickrema LC, Hor L, et al. The Structural Basis for Complement Inhibition by Gigastasin, a Protease Inhibitor from the Giant Amazon Leech. *J Immunol*. 2017;199(11):3883-3891. doi:10.4049/jimmunol.1700158

71. Cheng Y-C, Prusoff WH. Relationship between the inhibition constant (KI) and the concentration of inhibitor which causes 50 per cent inhibition (I50) of an enzymatic reaction. *Biochem Pharmacol*. 1973;22(23):3099-3108. doi:10.1016/0006-2952(73)90196-2

72. Perona JJ, Craik CS. Structural basis of substrate specificity in the serine proteases. *Protein Sci*. 1995;4(3):337-360. doi:10.1002/pro.5560040301

73. Perry AJ, Wijeyewickrema LC, Wilmann PG, et al. A molecular switch governs the interaction between the human complement protease C1s and its substrate, complement C4. *J Biol Chem*. 2013;288(22):15821-15829. doi:10.1074/jbc.M113.464545

74. Kardos J, Harmat V, Palló A, et al. Revisiting the mechanism of the autoactivation of the complement protease C1r in the C1 complex: Structure of the active catalytic region of C1r. *Mol Immunol*. 2008;45(6):1752-1760. doi:10.1016/j.molimm.2007.09.031

75. Schechter I, Berger A. On the size of the active site in proteases. I. Papain. *Biochem Biophys Res Commun*. 1967;27(2):157-162. doi:10.1016/S0006-291X(67)80055-X

76. Delong A, Hsu M, Kotsoris H. Estimation of cumulative number of post-treatment Lyme disease cases in the US, 2016 and 2020. *BMC Public Health*. 2019;19(1):1-8. doi:10.1186/s12889-019-6681-9

77. Mac S, da Silva SR, Sander B. The economic burden of lyme disease and the cost-effectiveness of lyme disease interventions: A scoping review. *PLoS One*. 2019;14(1):1-

17. doi:10.1371/journal.pone.0210280

78. NIAID. *Current Efforts in Lyme Disease Research.*; 2019. https://www.niaid.nih.gov/sites/default/files/NIAIDLymereport2015.pdf.

79. Locke JW. Complement evasion in Borrelia spirochetes: Mechanisms and opportunities for intervention. *Antibiotics*. 2019;8(2). doi:10.3390/antibiotics8020080

80. Caine JA, Lin YP, Kessler JR, Sato H, Leong JM, Coburn J. Borrelia burgdorferi outer surface protein C (OspC) binds complement component C4b and confers bloodstream survival. *Cell Microbiol*. 2017;19(12):1-14. doi:10.1111/cmi.12786

81. Kochi SK, Johnson RC. Role of immunoglobulin G in killing of Borrelia burgdorferi by the classical complement pathway. *Infect Immun*. 1988;56(2):314-321. doi:10.1128/iai.56.2.314-321.1988

82. Kraiczy P. Travelling between two worlds: Complement as a Gatekeeper for an expanded host range of lyme disease spirochetes. *Vet Sci*. 2016;3(2):1-15. doi:10.3390/vetsci3020012

83. Fischer JR, LeBlanc KT, Leong JM. Fibronectin binding protein BBK32 of the Lyme disease spirochete promotes bacterial attachment to glycosaminoglycans. *Infect Immun*. 2006;74(1):435-441. doi:10.1128/IAI.74.1.435-441.2006

84. Probert WS, Johnson BJB. Identification of a 47 kDa fibronectin-binding protein expressed by Borrelia burgdorferi isolate B31. *Mol Microbiol*. 1998;30(5):1003-1015. doi:10.1046/j.1365-2958.1998.01127.x

85. Hammerschmidt C, Koenigs A, Siegel C, et al. Versatile roles of CspA orthologs in complement inactivation of serum-resistant lyme disease spirochetes. *Infect Immun*. 2014;82(1):380-392. doi:10.1128/IAI.01094-13

86. Rossmann E, Kraiczy P, Herzberger P, et al. Dual Binding Specificity of a Borrelia hermsii -Associated Complement Regulator-Acquiring Surface Protein for Factor H and Plasminogen Discloses a Putative Virulence Factor of Relapsing Fever Spirochetes . *J Immunol*. 2007;178(11):7292-7301. doi:10.4049/jimmunol.178.11.7292

87. Kuipers A, Stapels DAC, Weerwind LT, et al. The Staphylococcus aureus polysaccharide capsule and Efb-dependent fibrinogen shield act in concert to protect against phagocytosis. *Microbiol (United Kingdom)*. 2016;162(7):1185-1194. doi:10.1099/mic.0.000293

88. Bennett KM, Rooijakkers SHM, Gorham RD. Let's tie the knot: Marriage of complement and adaptive immunity in pathogen evasion, for better or worse. *Front Microbiol*. 2017;8(JAN):1-17. doi:10.3389/fmicb.2017.00089

89. Garcia BL, Zwarthoff SA, Rooijakkers SHM, Geisbrecht B V. Novel Evasion Mechanisms of the Classical Complement Pathway. *J Immunol*. 2016;197(6):2051-2060. doi:10.4049/jimmunol.1600863

90. Harris CL, Pouw RB, Kavanagh D, Sun R, Ricklin D. Developments in anti-complement therapy; from disease to clinical trial. *Mol Immunol*. 2018;102(May):89-119.

doi:10.1016/j.molimm.2018.06.008

91. Carpanini SM, Torvell M, Morgan BP. Therapeutic inhibition of the complement system in diseases of the central nervous system. *Front Immunol*. 2019;10(MAR):1-17. doi:10.3389/fimmu.2019.00362

92. Food and Drug Administration. *October 10, 2008 Approval Letter - CINRYZE*.; 2008. http://wayback.archive-it.org/7993/20170723024211/https://www.fda.gov/BiologicsBloodVaccines/BloodBloodProducts/ApprovedProducts/LicensedProductsBLAs/FractionatedPlasmaProducts/ucm093602.htm.

93. Food and Drug Administration. *July 16, 2014 Approval Letter - RUCONEST*.; 2014. http://wayback.archive-it.org/7993/20170723024243/https://www.fda.gov/BiologicsBloodVaccines/BloodBloodProducts/ApprovedProducts/LicensedProductsBLAs/FractionatedPlasmaProducts/ucm405512.htm.

94. Food and Drug Administration. *Approval Letter*.; 2007. https://www.accessdata.fda.gov/drugsatfda_docs/nda/2007/125166s0000TOC.cfm.

95. Food and Drug Administration. *Supplement Approval*.; 2016. BLA 125166/S-422.

96. U.S. National Library of Medicine. ClinicalTrials.gov. https://clinicaltrials.gov/ct2/show/NCT03347396.

97. Grabarek Z, Gergely J. Zero-length crosslinking procedure with the use of active esters. *Anal Biochem*. 1990;185(1):131-135. doi:10.1016/0003-2697(90)90267-D

98. Timkovich R. Detection of the stable addition of carbodiimide to proteins. *Anal Biochem*. 1977;79(1-2):135-143. doi:10.1016/0003-2697(77)90387-6

99. Staros J V., Wright RW, Swingle DM. Enhancement by N-hydroxysulfosuccinimide of water-soluble carbodiimide-mediated coupling reactions. *Anal Biochem*. 1986;156(1):220-222. doi:10.1016/0003-2697(86)90176-4

100. Schuck P, Minton AP. Analysis of mass transport-limited binding kinetics in evanescent wave biosensors. *Anal Biochem*. 1996;240(2):262-272. doi:10.1006/abio.1996.0356

101. Glaser RW. Ag-Ab binding and mass transport by convection and diffusion to a surface-a 2D computer model of binding and dissociaiton kinetics. *Anal Biochem*. 1993;213:152-161.

102. GE Healthcare Life Science. Biacore TM Assay handbook. 2012:1-78. https://www.cytivalifesciences.co.jp/contact/pdf/BiacoreAssayHandbook.pdf.

103. Edwards PR, Gill A, Pollardknight DV, et al. Kinetics of Protein-Protein Interactions at the Surface of an Optical Biosensor. *Anal Biochem*. 1995;231(1):210-217. doi:10.1006/abio.1995.1522

104. Jain P, Arora D, Bhatla SC. Surface Plasmon Resonance Based Recent Advances in Understanding Plant Development and Related Processes. *Biochem Anal Biochem*.

2016;05(04). doi:10.4172/2161-1009.1000300

105. Paschkowsky S, Hsiao JM, Young JC, Munter LM. The discovery of proteases and intramembrane proteolysis. *Biochem Cell Biol*. 2019;97(3):265-269. doi:10.1139/bcb-2018-0186

106. Bond JS. Proteases: History, discovery, and roles in health and disease. *J Biol Chem*. 2019;294(5):1643-1651. doi:10.1074/jbc.TM118.004156

107. Mueller J. *Physiologie Und Wissenschaftliche Medicin*. Berlin: Archiv für Anatomie; 1836.

108. Northrop JH. Crystalline pepsin. *Science (80-)*. 1929;69(1796):580. doi:10.1126/science.69.1796.580

109. Northrop JH. CRYSTALLINE PEPSIN. *J Gen Physiol*. 1930;13(6):739-766. doi:10.1085/jgp.13.6.739

110. Bernal JD, Crowfoot D. X-ray photographs of crystalline pepsin. *Nature*. 1934;133(3369):794-795. doi:10.1038/133794b0

111. Northrop JH. *Crystalline Enzymes: The Chemistry of Pepsin, Trypsin, and Bacteriophage*. New York: Columbia University Press; 1939.

112. Drenth J, Jansonius JN, Koekoek R, Swen HM, Wolthers BG. Structure of papain. *Nature*. 1968;218(5145):929-932. doi:10.1038/218929a0

113. Radzicka A, Wolfenden R. Rates of uncatalyzed peptide bond hydrolysis in neutral solution and the transition state affinities of proteases. *J Am Chem Soc*. 1996;118(26):6105-6109. doi:10.1021/ja954077c

114. Oda K. New families of carboxyl peptidases: Serine-carboxyl peptidases and glutamic peptidases. *J Biochem*. 2012;151(1):13-25. doi:10.1093/jb/mvr129

115. Perona JJ, Hedstrom L, Rutter WJ, Fletterick RJ. Structural Origins of Substrate Discrimination in Trypsin and Chymotrypsin. *Biochemistry*. 1995;34(5):1489-1499. doi:10.1021/bi00005a004

116. Blow DM, Birktoft JJ, Hartley BS. Role of a buried acid group in the mechanism of action of chymotrypsin. *Nature*. 1969;221(5178):337-340. doi:10.1038/221337a0

117. Ma W, Tang C, Lai L. Specificity of trypsin and chymotrypsin: Loop-motion-controlled dynamic correlation as a determinant. *Biophys J*. 2005;89(2):1183-1193. doi:10.1529/biophysj.104.057158

118. Perona JJ, Craik CS. Evolutionary divergence of substrate specificity within the chymotrypsin-like serine protease fold. *J Biol Chem*. 1997;272(48):29987-29990. doi:10.1074/jbc.272.48.29987

119. De Veer SJ, Wang CK, Harris JM, Craik DJ, Swedberg JE. Improving the Selectivity of Engineered Protease Inhibitors: Optimizing the P2 Prime Residue Using a Versatile Cyclic Peptide Library. *J Med Chem*. 2015;58(20):8257-8268. doi:10.1021/acs.jmedchem.5b01148

120. Tsukada H, Blow D. Structure of alpha-chymotrypsin refined at 1.68 A resolution. *J Mol Biol*. 1985;184:703-711. http://scholar.google.com/scholar?hl=en&btnG=Search&q=intitle:Structure+of+alpha-Chymotrypsin+Refined+at+1.68A+Resolution#0.

121. PerkinElmer. *Alpha Assays Protein:Protein Interactions*.; 2016.

122. Eglen RM, Reisine T, Roby P, et al. The Use of AlphaScreen Technology in HTS: Current Status. *Curr Chem Genomics*. 2008;1:2-10. doi:10.2174/1875397300801010002

123. Gorshkov K, Chen CZ, Xu M, et al. Development of a High-Throughput Homogeneous AlphaLISA Drug Screening Assay for the Detection of SARS-CoV-2 Nucleocapsid. *ACS Pharmacol Transl Sci*. 2020;3(6):1233-1241. doi:10.1021/acsptsci.0c00122

124. Beaudet L, Rodriguez-suarez R, Caron M, et al. Application Notes Advertising Feature. 2008;(December):8-9. http://www.nature.com/naturemethods.

APPENDIX A: Surface Plasmon Resonance

Surface plasmon resonance (SPR) is a powerful biochemical technique used for a variety of means including kinetic and steady state analyses of biomolecular interactions. SPR experiments begin with the immobilization of the protein ligand of interest either coupled or affinity captured onto a biosensor chip. These chips contain gold surfaces on which different coatings for ligand binding are available. The coupling chemistry performed in this work was completed using amine coupling. First a chip coated with carboxymethyl dextran (CMD) is washed and equilibrated. The carboxymethyl group is then subjected to activation of its carboxyl group by a mixture of NHS (N-hydroxysuccinimide) and EDC (N-ethyl-N'-(dimethylaminopropyl) carbodiimide) to create NHS esters, which encourages the formation of the acyl intermediate with an amine[97–99]. Ligand associated primary amines, such as lysine and N-terminal residues, on the ligand are then activated by ensuring the pH of the solution is below the isoelectric point of the ligand of interest. This uniform positive charge increases the charge-charge interactions at the surface, which increases the amount of ligand to be covalently crosslinked through the formation of an amide bond to the carboxylic acid. Control of this step is critical for SPR experimentation as if the immobilization level is too low signal is restricted. Alternatively, if the immobilization level is too high the movement of the analyte from the buffer to the surface, also known as mass transport, confers problems with diffusion of analyte from the soluble phase causing unintended masking of interactions at the surface[100,101]. Finally, a short two carbon molecule with properties of an alcohol and a primary amine, ethanolamine, is used to quench unreacted carboxyl intermediates and return the surface to a stable state.

Subsequent experimentation may then be performed on the surface for ligand analyte interactions. Two general approaches can be taken for analyses, Kinetic or steady state

experimentation. Kinetic analyses are used to determine association rate constant (k_a, 1/Ms) and dissociation rate constant (k_d, 1/s), which can be used to determine the dissociation constant (K_D, M)[102]. Steady state analysis is used to describe the interaction at equilibrium, where the response at equilibrium (R_{eq}) is dependent on the concentration of complex formed[102]. Steady state affinity can therefore be determined when R_{eq} approaches half R_{max} this concentration serves as an equivalent dissociation constant, K_D, but does not take in the dynamics of the kinetic interaction[102]. To determine kinetic constants, various concentrations of analyte in running buffer are injected over a surface. Interaction between surface bound ligand and soluble analyte results in a protuberance at the surface of a metal surface. The change in mass at the surface disrupts surface plasmons, which upon interaction results in a difference in the evanescent wave which can be measured as a difference in refractive index (**Fig A1**). Due to the nature of these interactions neither species needs to be labelled and high sensitivity and specificity is obtained given the proper experimental set up. Experimentation performed in this study was performed using multi-cycle kinetics where a normal set up contains several doses of analyte, which are injected over the surface and subsequently regenerated using a high-salt low-pH buffer to release analytes from non-covalent interactions with ligands. Upon regeneration the surface is returns to baseline levels and is ready for the next injection of analyte. Subsequent analysis of binding events is performed using various models of binding appropriate for the mechanism of interaction between the analyte and ligand[102,103]. SPR remains a key for the description of biophysical interactions as small as 100 Da[102].
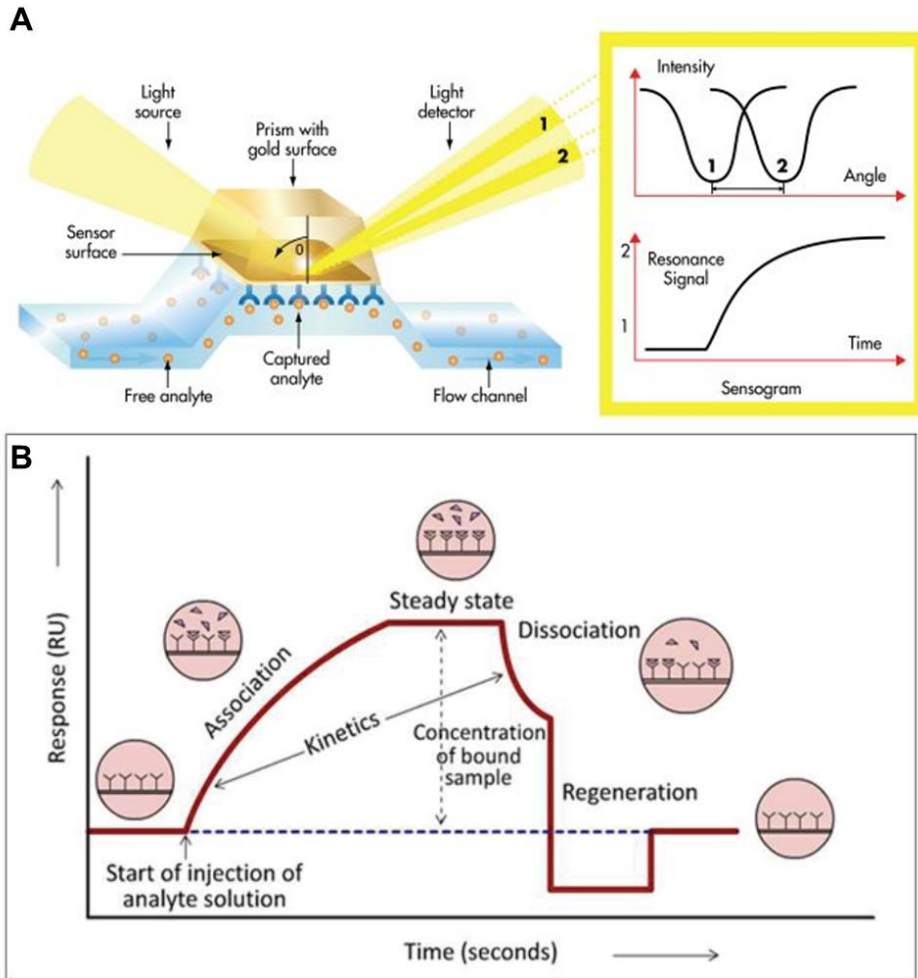
Figure A1. Diagram of mechanisms and principles of SPR. A) Upon grating of a light source

SPR uses total internal reflection (TIR) passed through a prism, which changes the lights

intensity at a specific angle resulting in a difference in response. This angle is proportional to the

mass change of a surface bound ligand binding to an injected analyte (Bruker.com/surface-

plasmon-resonance). **B)** Model of an SPR sensorgram resulting from ligand binding of analyte

with difference in resonance units (RU) over time allows us to determine kinetic parameters

correlating to association (k_a), dissociation (k_d), and the point at which the ligand reaches

equilibrium with the concentration of analyte, also known as steady state[104].

Appendix B: Chymotrypsin-like serine proteases

Found in all forms of life, including viruses, proteases are the subject of much research and have incredible impact on biological systems[72,105,106]. Credited with the isolation of the first protease was Theodor Schwaan, who noticed the ability of a mysterious component, which he named pepsin, that aided in the digestion of egg albumin in gastric juices nearly 200 years ago[105,107]. However, it wasn't until 1929 that John Northrop first crystallized pepsin and subsequently his methods led to the first ever x-ray photograph of a protein in 1934 by Bernal and Crowfoot[108–110]. Although the structures would not come until much later Northrop crystallized many hallmark proteases such as chymotrypsin, trypsin, and pepsinogen altogether his work earning a Nobel Prize in Chemistry in 1946[105,111]. 22 years after his receipt of the Nobel Prize, seminal work performed by Drenth et al in 1968 solved the first protease structure of the cysteine protease papain[112]. Since then scientists have continued research on the mechanisms that proteases use to recognize substrates, factors that result in their activation, and subsequent control of activated proteases.

Proteases are enzymes which catalyze the hydrolysis of peptide bonds, thereby resulting in degradation of their targets[113]. There are seven main groups of proteases that are named according to unique attributes that reside in that group – cysteine proteases, threonine proteases, aspartic proteases, glutamic proteases, metalloproteases, asparagine peptide lyases, and serine proteases[114]. Perhaps one of the most studied groups is the serine proteases, which are further characterized in three classes trypsin, chymotrypsin, and subtilisin like[72,115]. The three classes contain high homology in both secondary and tertiary motifs, which all perform the same chemical reaction. First a target peptide interacts with substrate specificity sites on the enzyme at which point a specific spatial arrangement of amino acids, known as a catalytic triad. The

catalytic triad of serine histidine and aspartic acid coordinate the peptide to create an acyl intermediate promoting the leaving of the non-acylated residues[72,116]. Deacylation then occurs through the coordination of water and formation of a carboxylic acid (**Fig A2A**)[116].

Recognition of substrates occur through both the catalytic site of the enzyme and regions of specificity dictated by loops surrounding the catalytic site[72]. In the active site of the enzyme lies substrate specificity pockets which correspond to the interactions they make with the cleavage peptide. The numbering scheme starts with S_n the last interaction on the enzyme side of one leaving peptide and ending with S_n' this is illustrated in (**Fig A2B**)[75]. Substrate specificity pockets are formed upon the activation of the enzyme serving as an internal mechanism of regulation against unintended peptide cleavage. Overall these subsites contribute to the main difference in chymotrypsin, which cleaves C-terminal bonds next to aromatic residues, and trypsin which has preference toward C-terminal basic amino acids[117]. Recognition of substrates is also assisted in part by 8 surface loops, which accompanied by 2 β-barrels makes up the canonical trypsin fold[118]. These loops are labelled according to their position in trypsin and have been assigned several functions over the years with main determinants of importance residing in deletions and insertions (**Fig A2C**)[72]. Insertions and deletions in surface loops also promote differential intramolecular interactions which influence substrate specificity both contributing to the formation of mature S sites and the recognition of substrates outside of the active sites[118,119].
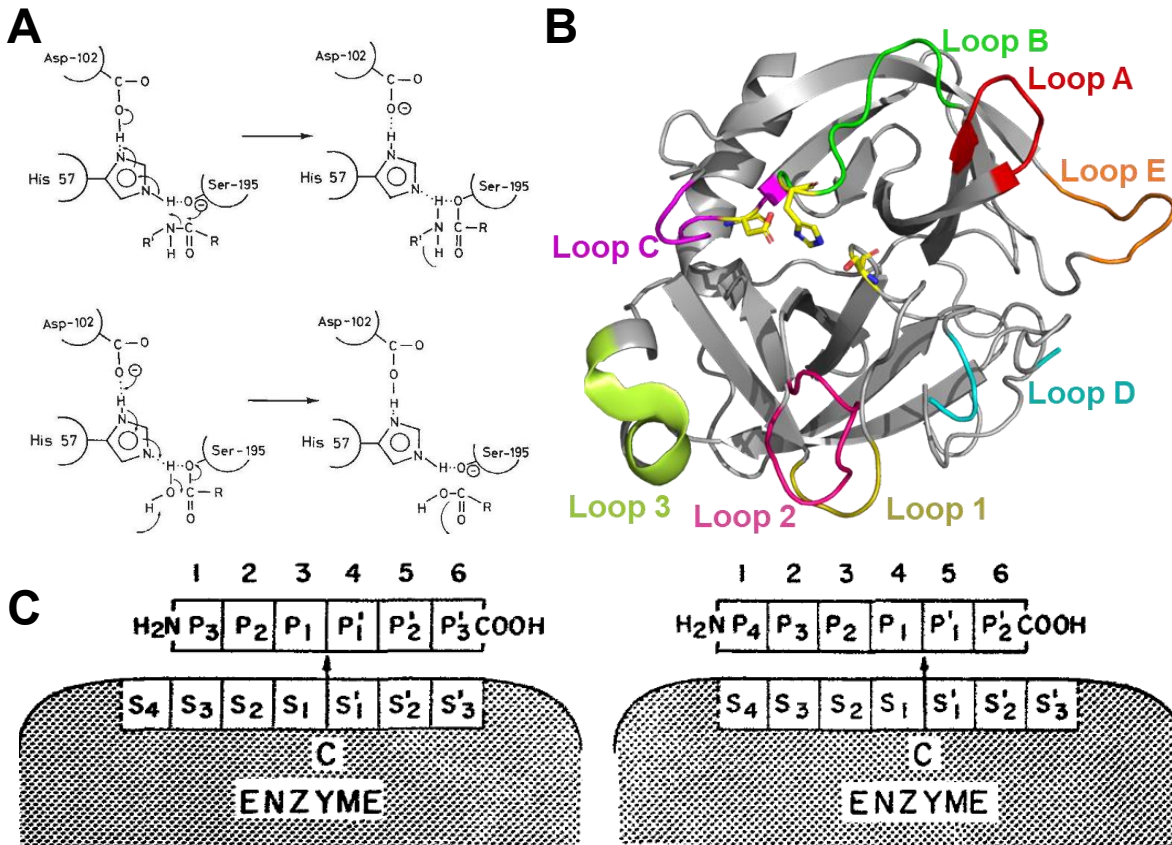
Figure A2. Schematic of chymotrypsin-like serine protease mechanism of action. **A)** Catalytic mechanism of action of the serine protease cleavage of a peptide. Coordination of P1 and P1' residues causes nucleophilic attack of the carbonyl on P1 resulting in formation of an acyl intermediate (Top). Subsequent deacylation is performed with hydrolysis to complete cleavage and release products (Bottom). **B)** Cartoon model of bovine α-chymotrypsin (PDB: 4CHA) with loops colored according to trypsin numbering[120]. Catalytic triad His-57, Asp-102, and Ser-195 are colored in yellow as stick models. **C)** Model of peptide enzyme interaction nomenclature. Enzyme subsites are labelled with "S" where corresponding peptide residues "P" the cleavage site "C" denotes the site of peptide cleavage. Residues past the P1 and S1 are denoted with primes to indicate leaving groups. Panel (**A**) was reproduced from Blow et al. 1967 and (**C**) was reproduced from Schechter and Berger, 1967[75,116].

Appendix C: Amplified Luminescence Proximity Homogenous Assay

Amplified luminescence proximity homogenous assay (ALPHA) is a no wash biochemical technique developed by Perkin-Elmer which uses a bead-based technology to assess biomolecular interactions between two species[121]. This assay uses a two-bead system, Acceptor and Donor, which react when in close (< 200 nm) proximity. Biomolecules of interest are conjugated or otherwise associated with the surface of individual beads and upon interaction will bring the beads into proximity. At steady state there should be an equal number of biomolecular interactions occurring on the surface of these beads. The beads are then subjected to illumination by a laser at 680 nm, which creates a singlet oxygen species using a photosensitizer on the donor bead, phthalocyanine. This reactive singlet oxygen has a half-life of approximately 4 µsec, however if the oxygen is in close proximity to an acceptor bead it reacts with thioxenes producing fluorophores that can be measured at 615 nm[121]. The final measurement is taken as an accumulation of ALPHA signal (counts), in 140 ms making the ALPHA assay an incredibly sensitive assay format.

In a normal experiment, an 8 x 8 screen of protein concentration is performed to find the optimal amount of each protein to add to a recommended 20 µg/mL of each bead. One can take advantage of this grid screen approach to select a ratio of at least 10 ligand to 1 protein in order for the approximations made by Cheng and Prusoff, IC_{50} approximates K_D, to be effective[71,121]. Reactions are performed in 25 µL reaction volumes in half area ALPHA plates which block out contaminating light for improved signal. Reactions are then considered steady state at 1 hr of incubation at room temperature. Experiments are then read on an ALPHA compatible plate reader, such as the Perkin-Elmer Ensight.

Experiments are generally performed in one of two ways, direct or indirect. Direct

ALPHAs measure the binding of the two proteins bound at steady state (**Fig A3A**). This

interaction is then introduced to a competitor, which interrupts the interaction resulting in loss of

signal. Alternatively, an indirect ALPHA can be used to determine whether simultaneous binding

is able to occur. Two biomolecules which do not bind each other but have a common ligand can

create an ALPHA signal if both molecules interactions are non-overlapping (**Fig A3B**). The high

level of versatility and small sample size makes it a perfect candidate for the characterization of

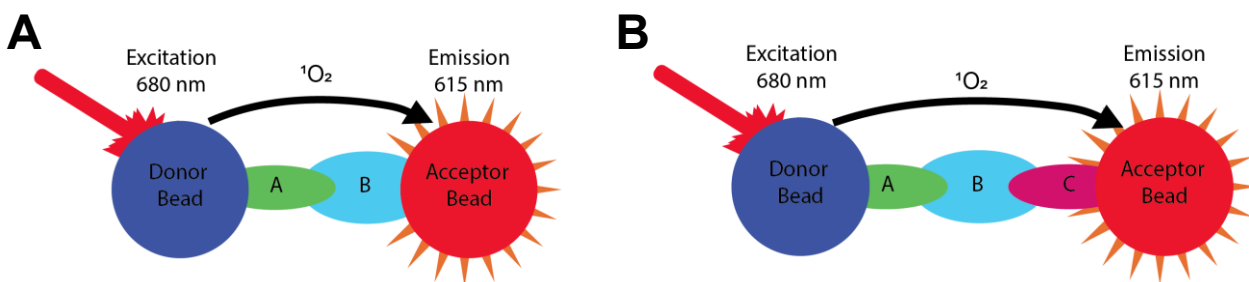drug-target interactions as well as small molecules[122–124].

Figure A3. Model of direct and indirect ALPHA signal transduction. A) Model of direct ALPHA interaction between biomolecules A (green) associated with the donor bead and B (cyan) associated with the acceptor bead allows for direct measurement of interaction of A and B. **B)** Model of indirect ALPHA interaction with biomolecule A (green) associated with the donor bead and biomolecule C (pink) associated with the acceptor bead. Although both biomolecules do not interact on their own addition of biomolecule B (cyan) mediates signal transduction.